Cell-Type Specific Interrogation of CeA *Drd2* Neurons to Identify Targets for Pharmacological Modulation of Fear Extinction.

Kenneth M. McCullough, PhD[1,2], Nikolaos P. Daskalakis[1], Georgette Gafford, PhD[2], Filomene G. Morrison PhD [1,2], and Kerry J. Ressler, MD, PhD[1,2]

[1] Division of Depression & Anxiety Disorders,
McLean Hospital, Department of Psychiatry, Harvard Medical School, Boston MA
[2] Behavioral Neuroscience, Department of Psychiatry
and Behavioral Sciences, Emory University, Atlanta, GA

Corresponding Author:
Kerry Ressler, MD, PhD
Mclean Hospital
Oaks Building 104b, Mailstop 212
115 Mill Street
Belmont, MA 02478-1064
TEL: 617.855.4210 FAX: 617.977.4213
EMAIL: kressler@mclean.harvard.edu

Pages: 21

Figures: 5

Tables: 4

Supplementary: 8

Acknowledgements:

Support was provided by NIH (R01 MH108665-01) and Cohen Veteran Biosciences foundation.

The authors declare no competing financial interests.

Abstract

Behavioral and molecular characterization of cell-type specific populations governing fear learning and behavior is a promising avenue for the rational identification of potential therapeutics for fear-related disorders. Examining cell-type specific changes in neuronal translation following fear learning allows for targeted pharmacological intervention during fear extinction learning, mirroring possible treatment strategies in humans. Here we identify the central amygdala (CeA) *Drd2*-expressing population as a novel fear-supporting neuronal population that is molecularly distinct from other, previously identified, fear-supporting CeA populations. Sequencing of actively translating transcripts of *Drd2* neurons using translating ribosome affinity purification (TRAP) technology identifies mRNAs that are differentially regulated following fear learning. Differentially expressed transcripts with potentially targetable gene products include *Npy5r, Rxrg, Adora2a, Sst5r, Fgf3, Erbb4, Fkbp14, Dlk1,* and *Ssh3*. Direct pharmacological manipulation of NPY5R, RXR, and ADORA2A confirms the importance of this cell population and these cell-type specific receptors in fear behavior. Furthermore, these findings validate the use of functionally identified specific cell populations to predict novel pharmacological targets for the modulation of emotional learning.

Introduction

The amygdala is a mediator of the acquisition and expression of learned associative fear[1,2]. Composed primarily of GABAergic medium spiny neurons, the central amygdala (CeA) is intimately involved in controlling the expression of fear related behaviors[3,4]. Each of the CeA's three main sub-nuclei (lateral capsular (CeC), lateral (CeL), and medial (CeM)) play distinct roles in specific behaviors and contain molecularly distinct sub-populations that have further behavioral specializations[5-10]. In the present set of experiments, we utilized Pavlovian fear conditioning, a paradigm used extensively for studying associative fear memories formed by the pairings of conditioned stimuli (CS; e.g. a tone) and unconditioned stimuli (US; e.g. a mild foot shock)[11-13]. Learned fearful associations may be 'extinguished' with additional unreinforced presentations of the CS alone, a process that closely resembles the clinical practice of exposure therapy used in treating individuals with PTSD. A promising area of treatment in PTSD includes the pharmacological enhancement of exposure-based therapies[14]. The aim of this study is to harness cell-type specific molecular techniques in order to identify more specific and effective pharmacotherapies for the treatment of fear-related disorders.

Foundational research as well as more recent analyses highlight the striatum-like nature of the central amygdala[15]. Striatal dopamine receptor 1 (*Drd1*) populations (direct pathway neurons) promote movement, while dopamine receptor 2 (*Drd2*) populations (indirect pathway neurons) inhibit movement[16,17]. Within the posterior CeA, it has been reported that corticotropin releasing factor (*Crh*), tachykinin 2 (*Tac2*), somatostatin (*Sst*), and neurotensin (*Nts*) expressing populations are contained within the larger *Drd1* expressing neuron population that promote directed motivational behaviors under certain conditions [18,19]. Conversely, within the anterior CeC, the protein kinase C-δ (*Prkcd*) and calcitonin receptor-like (*Calcrl*) co-expressing population has been reported to be a sub-population of *Drd2* neurons mediating defensive behaviors or inhibiting motivated behaviors[19,20]. Given its potential role in fear behavior, the CeA *Drd2* expressing population is a high value target for translational investigation.

The dopaminergic system is well known for its role in appetitive learning; however, more recently it has been recognized for its importance in fear acquisition and fear extinction learning[21-23]. Perturbations in the dopaminergic system have been implicated in the disease etiologies of several human pathologies ranging from Parkinson's disease to schizophrenia, depression and posttraumatic stress disorder (PTSD)[24-26]. Although the dopamine receptor 2 (D2R) is clearly involved in fear acquisition and fear extinction learning, the literature to date has been equivocal on the role of D2R in the CeA, as different study designs demonstrate D2R antagonist administration may lead to conflicting effects[27-29]. In the present study, we separate the role of CeA *Drd2*-expressing neurons in fear behavior from that of receptor activity of D2R itself, and in doing so, indentify a large number of alternative gene targets that are modulated by fear learning.

The present study takes the most translationally direct approach by behaviorally and molecularly characterizing the CeA *Drd2* neuronal population, examining translational changes in this population following a fear learning event, and then pharmacologically manipulating identified targets at a clinically relevant time-point, during fear extinction. Molecular characterization of this population clearly identifies it as a unique population that is largely non-overlapping with other, previously described CeA populations. Direct chemogenetic enhancement of excitability in CeA *Drd2* neurons resulted in significantly enhanced fear expression. Translating ribosome affinity purification (TRAP) and sequencing of actively translated RNAs in the *Drd2* neuron population following fear conditioning yielded a diverse set of genes differentially regulated by behavior[30]. These differentially regulated genes included *Adora2a*, *Rxrg, Sst5r, Npy5r, Fgf3, Erbb4, Gpr6, Fkbp14, Dlk1* and *Ssh3*. Using the Druggable Genome database, genes with known pharmacological interaction partners were chosen and pharmacologically manipulated at a clinically relevant time point to oppose fear conditioning dependent changes, during fear extinction. Consistent with the identification of the *Drd2* expressing population as a fear expression supporting population, blockade of $A_{2A}R$ ($G_{\alpha s}$) or NPY5R ($G_{\alpha i}$) during fear extinction suppressed and enhanced fear expression respectively. Additionally, activation of RXR enhanced fear extinction consolidation. Together these data provide promising new targets for understanding and manipulating fear processes, and also demonstrate the power of identifying novel pharmacological targets through the use of cell-type specific approaches to amygdala circuit function.

Results:

Drd2 defines a distinct CeA population.

Many molecularly distinct subpopulations have been identified across the CeA. Using RNAScope technology, we performed fluorescence *in situ* hybridization (FISH) in order to examine the *Drd2* population in relation dikkopf-related protein 3(*Dkk3*), dopamine receptor 1a (*Drd1a*), adenosine A2A receptor (*Adora2a*), corticotropin releasing factor (*Crh*), neurotensin (*Nts*), protein kinase C-δ (*Prkcd*), somatostatin (*Sst*), and tachykinin 2 (*Tac2*). Within the striatum, *Drd1a* and *Drd2* have expected intermingled, non-overlapping, expression patterns (Figure 1A-F). *Dkk3* strongly labels a population of BLA primary neurons. *Drd1a* strongly labels intercalated cell masses (ITC), especially the main intercalated island, and weakly labels some BLA cells. *Drd2* does not label any BLA or ITC cells. Within the CeA at anterior positions, *Drd2* primarily labels populations in the CeC and CeL with lower expression within the CeM, while *Drd1* primarily labels populations in the CeL and CeM with less expression within the CeC [2,31,32]. At higher magnification it is clear that within the CeA *Drd1a* and *Drd2* maintain their

non-overlapping expression with very few identifiable co-expressing cells (Figure 1G-L). *Drd2* is known to strongly co-express with *Adora2a* in the striatum. Similarly, we find an almost complete co-expression of *Drd2* and *Adora2a* within amygdala neurons.

The anterior to posterior (A/P) position within the CeA has emerged as a strong potential variable when examining the behavioral functions of CeA neurons[19]. Therefore, the distribution of *Drd2, Drd1a,* and *Adora2a* expressing cells was examined across the length of the CeA (Supplemental Figure 1 A-X). Consistently, *Drd2* and *Drd1a* label non-overlapping populations, while *Drd2* and *Adora2a* label almost entirely overlapping populations with some single labeled cells found at the far ventral portion of the CeC. At anterior positions (A/P: -.82 to -1.2), *Drd2* strongly labels large populations within the CeC and CeL and to a lesser extent the CeM (Supplemental Figure 1A). Likewise, *Drd1a* labels populations within the CeL and CeM and many fewer cells in the CeC. At more posterior positions (A/P: -1.3 to -1.6) labeled cell distributions are less defined; the CeC, CeL and CeM are sparsely labeled aside from a strongly labeled dorsal *Drd2/Adora2a* population that appears to be contiguous with the striatum. Interestingly, the posterior CeA, especially posterior CeL, which contains the densest labeling for *Crh, Nts, Sst, Prkcd,* and *Tac2,* is only sparsely labeled with *Drd1a* (Supplemental Figure 1. D, H, L, P, T, X and Figure 2 M, N, Q, R).

To statically assess the extent to which the *Drd2* population overlaps with markers of other identified fear-related CeA populations, co-expression of *Drd2* with *Crh, Nts, Sst, Prkcd,* and *Tac2* was quantitatively assessed across the A/P axis of the CeA (Figure 2 A-Z and Supplemental Figure 2 A-J). Anterior CeA was considered to be between -.8 and -1.2 A/P while posterior CeA was considered as between -1.3 and -1.6. Posterior to approximately -1.6 was not examined, as the CeM is absent. Positive expression within a cell was visually scored as having five or more labeled puncta within twice the diameter of the nucleus. Single labeled images were scored then identified nuclei were overlaid and counted for none, single and double labeling.

Within the anterior CeA, *Drd2* was not found to extensively co-express with any other population examined (Figure 2B). Within the anterior CeL and CeM *Drd2* co-expressed significantly more with *Crh* and *Tac2* respectively compared to other markers, although total co-expression was low at 19.3% and 13.1% of *Drd2* positive cells co-localized with *Crh* and *Tac2*, respectively (Figure 2 C, G, K, O, S, W and Supplemental Figures 2C and G). Within the posterior CeC and CeL, *Drd2* co-expressed more with *Prkcd* than any other marker (36.7% and 31.5% of *Drd2* cells in the CeC and CeL, respectively); however this represented a relatively low percentage of total *Prkcd* positive cells (13.9% and 10.1% of *Prkcd* positive cells in the CeC and CeL, respectively)(Supplemental Figure 2B). Staining for *Prkcd* was found beginning in the anterior ventral CeC forming a contiguous population to a more dorsal position posteriorly where the traditionally reported CeC and CeL population is found (Figure 2L & M).

Chemogenetic activation of CeA *Drd2* neurons enhances fear expression.

To determine the precise role of the *Drd2*-expressing population in fear extinction, we directly manipulated these neurons during extinction using designer receptors exclusively activated by designer drugs (DREADDs)[33]. Drd2-Cre (B6.FVB(Cg)-Tg(Drd2-Cre)ER43Gsat/Mmucd) mice and non-Cre expressing littermate controls were infected bilaterally with a Cre-dependent Gs-coupled DREADD virus (Figure 3A-C). Gs-DREADD expression was visualized through its mCherry tag (Figure 3B and C). Three weeks following infection, mice were mildly fear conditioned with 5 CS/US (0.4 mA US footshock) pairings to

avoid ceiling effects (Figure 3D). A trend towards increased freezing in the Drd2-Cre mice was found during conditioning; if this represents a true finding it may have been caused by leakage of the Gs-DREADD; however, freezing during the final CS/US paring was very similar between both groups, suggesting no differences in overall fear learning. 30 minutes prior to the extinction session (15 CS), all mice were injected with CNO (1 mg/kg, i.p. in saline). Mice that expressed Cre-recombinase and thus expressed the Gs-DREADD in *Drd2* neurons exhibited significantly more freezing to the tone throughout the extinction session. Importantly, 24 h later, after a wash-out period when DREADDs were no longer active (previous research has shown that wash-out is 6-10 h[34,35,36]), Gs-DREADD expressing mice again displayed significantly more freezing to the CS compared to controls during a 30 CS extinction retention session. The rate of extinction of both groups in the initial extinction session did not significantly differ, suggesting that the enhancement in freezing during the second extinction session was likely due to blockade of extinction consolidation.

Characterization of dynamic mRNA changes in *Drd2* cells following fear conditioning.

To further characterize the *Drd2*-expressing population, we next examined expression changes in *Drd2* neurons following fear conditioning. Transcripts were examined following fear conditioning based on the expectation of this time point predicting the direction of protein expression levels 24-hours later prior to fear extinction. Additionally, we expected that modulation of fear learning precipitated molecular changes may lead to decreased fear expression or enhanced extinction. To identify actively translating mRNA transcripts, TRAP protocol was utilized[30]. The *Drd2*-Cre mouse line was crossed with the floxed-stop-TRAP (B6.129S4-Gt(ROSA)26Sortm1(CAG-EGFP/Rpl10a,-birA)Wtp/J) line to generate a double transgenic line, *Drd2*-TRAP. Expression of the L10a-GFP transgene closely recapitulated our observed expression patterns of *Drd2* (Supplemental Figure 3)[37-39]. Next, animals were either fear conditioned (5 CS/US tone-shock pairings with 0.5 sec, 0.65 mA foot shock US) or exposed to the tone CS in the chamber in the absence of any US. Fear conditioned animals exhibited expected increases in freezing responses to the CS (Supplemental Figure 4A). Animals were then sacrificed 2 h following behavior, micropunches centered over the CeA were collected, and TRAP was performed to obtain isolated mRNA from *Drd2* neurons (Figure 3E). High quality RNA was retrieved from the TRAP protocol (RIN=8.5-10). To verify the specificity of RNA pull-down, qPCR analysis of samples was performed to compare bound versus unbound samples. Ribosomal subunit 18S was found at higher levels in the bound fraction compared to the unbound fraction, confirming enrichment for ribosomes (Supplemental Figure 5A). When expression levels of *Drd2* and *Drd1a* were compared in ribosomal bound and unbound fractions, the bound fraction had a large enrichment of *Drd2* versus *Drd1a* transcripts when compared to the unbound fraction (Supplemental Figure 5B) [40-42]. Ribosomes specifically expressed in *Drd2* neurons were successfully pulled down and RNA collected from these pull-downs demonstrated expected characteristics of *Drd2* neurons; strong expression of *Drd2* and weak expression of *Drd1a*.

Sequencing of RNA collected from *Drd2* neuron ribosomes revealed genes dynamically regulated following fear conditioning, many of which have been previously reported to be involved in fear and anxiety-like behaviors (Figure 3F). False discovery rate (FDR) adjusted p-values were calculated and FDR of 5% and fold-change of $2^{\wedge 0.5}$ cut-offs were set(Full list of differentially expressed genes is in Supplemental Table 1). Using, the Mouse Gene Atlas dataset, initial analysis using Enrichr confirms amygdala specificity of pull-down and gene change (Supplemental Table 2)[43]. Further enrichment analysis using Jensen Compartments dataset

confirms neuronal specificity of pull down and gene change (Supplemental Table 3). Consistent with activity dependent gene changes, MetaCore Gene Ontology Processes identifies neuronal developmental and adenylate cyclase related processes as highly significantly recruited by fear conditioning (Figure 4A). MetaCore Gene Ontology Diseases identifies Schizophrenia and nervous system diseases as gene categories most related to gene changes in *Drd2* neurons (Figure 4B). Interestingly, GSEA identified gene group differences in the entire RNA-seq dataset as most concordantly similar, but in the opposite direction to two gene data sets identified in hippocampus and mPFC of humanized 22q11.2 deletion model of Schizophrenia (Supplemental Figure 6)[44,45]. This is informative for interpreting the enrichment of our top FDR-significant genes with Schizophrenia disease set by MetaCore. Weighted network analysis was completed to examine differential expression of *Drd2* genes in the context of human PTSD. Using GeneMANIA Cytoscape, differentially expressed transcripts were mapped into a self-organizing weighted network, where all of the genes were interlinked at multiple levels (co-expression, physical interactions, common pathway) (Figure 4C)[46,47]. Over-all gene network analysis reveals that differentially regulated genes are primarily co-expressed and are part of common ontologies without belonging to a single dominant pathway. To identify potential targets for pharmacological manipulation, differentially expressed genes were examined for the availability of agonists or antagonists using MetaCore Drugs for Drug targets tool (Supplemental Table 4). Finally, potential drug targets were examined in the literature for being high quality, blood-brain barrier penetrant, agonists or antagonists. Using this identification approach, inclusive of our *a priori* interest in *Adora2a* among other potential *Drd2*-neuron specific genes (above studies), *Npy5r,* and *Rxrg* were selected for further pharmacological examination[48-51]. Additional markers found to be modulated with fear learning that may be of further interest also include *Sst5r, Fgf3, Erbb4, Gpr6, Fkbp14, Dlk1* and *Ssh3.*

Based upon the altered translational activity in *Drd2* neurons following fear conditioning, one potential route to enhance fear extinction is to pharmacologically manipulate the activity of the identified translated protein products. ADORA2A, NPY5R, and RXR were chosen as potential targets for pharmacological modulation of fear extinction, as they were robustly differentially expressed in the *Drd2* fear-regulating neuronal population, and they have well-understood mechanisms of action, making them attractive targets for pharmacological manipulation of fear extinction.

Manipulation of ADORA2A, NPY5R, and RXR recapitulates the role of *Drd2* neurons in fear behavior

Agonists and antagonists targeting ADORA2A, NPY5R, and RXR receptors were chosen from the literature (Figure 5A)[52]. *Adora2a* was an attractive candidate for further inquiry and was chosen for initial characterization based on a number of reasons; 1) it has previously been shown to almost entirely co-express with *Drd2* (Figures 1G-L and 2) within the amygdala, and 2) several pharmacological agents targeting ADORA2A are currently in clinical trials or have been approved for use in humans[53,54]. The highly selective ADORA2A antagonist, istradefylline, is selective for ADORA2A over ADORA1 with a Ki of 2.2 and 150 nM respectively[55,56].

To examine the effect of ADORA2A antagonism on fear extinction three cohorts of mice were fear conditioned(5 CS/US, 0.65 mA foot shock)(Figure 5B and C). Twenty-four hours following fear conditioning, and 30 minutes prior to fear extinction, mice were injected with istradefylline (3 mg/kg) (group I/V) or vehicle (10% DMSO, 1% NP-40 in saline i.p.) (groups V/V and V/I) (Figure 5B). Additionally, immediately following fear extinction (15 CS) mice

were again injected with istradefylline (3 mg/kg) (group V/I) or vehicle (groups I/V and V/V). Injection of istradefylline but not vehicle prior to fear extinction (15 CS, Extinction 1) greatly decreased freezing during extinction training when drug was on-board (Figure 5D). Twenty-four hours later, following drug clearance, mice that had previously been injected with istradefylline prior to fear extinction, but not those injected following it, expressed significantly less freezing during a second extinction session (15CS, Extinction 2). These data suggest that blockade of ADORA2A during fear extinction, but not during extinction consolidation, is sufficient to enhance fear extinction learning.

To further examine the role of ADORA2A in fear consolidation, a separate cohort of mice was fear conditioned (5 CS/US, .65 mA) and given injections of istradefylline (3 mg/kg, i.p.) or vehicle directly following the fear conditioning training session (5 CS/US, 0.65 mA foot shock), (Figure 5 E and F). Although there was a trend towards decreased fear expression during a fear extinction (15 CS) session 24 hours later in mice treated with istradefylline, no significant effect of ADORA2A blockade on fear consolidation was detected.

Istradefylline is a potential drug treatment for Parkinson's disease, thus it is possible that locomotor effects obscured the effects of drug on fear behavior; therefore, two cohorts of mice were tested for locomotor and anxiety-like behaviors in an open field, and acoustic startle responses on consecutive days (Figure 5H). Injection of istradefylline (3 mg/kg) but not vehicle significantly increased the distance traveled in the open field (Figure 5I); however 24 hours later the distance traveled had returned to pre-treatment levels. Importantly, increased distance traveled was not accompanied by any anxiogenic or anxiolytic effects in the open field. The decreased locomotor activity across days is likely due to habituation to the chamber context. Finally, istradefylline acutely decreased baseline acoustic startle; however this effect was not present 24 hours later when startle amplitude returned to pre-treatment levels. Together, these data suggest that the effects of istradefylline in enhancing extinction retention tested 24 hours after drug administration are unlikely the result of alterations in locomotion or effects on anxiety-like behavior, per se.

NPY5R and RXR were additional identified targets that were examined for pharmacological enhancement of fear extinction. Velneperit antagonizes NPY5R, while Bexarotene is a RXR agonist (Figure 5L). A cohort of animals was fear conditioned (5 CS/US, 0.65 mA foot shock) (Supplemental Figure 7A). Twenty-four hours later, 90 minutes prior to fear extinction (15 CS), animals were given injections of Velneperit (100 mg/kg) or Vehicle (DMSO) (Figure 5M). Animals treated with Velneperit (NPY5R antagonist) expressed significantly more freezing than animals injected with vehicle (Extinction 1). Twenty-four hours later during a second extinction session (Extinction 2), no difference between groups was detected. Another cohort of animals was fear conditioned (5 CS/US, 0.65 mA foot shock) (Supplemental Figure 7B), and 24 hours later, 90 minutes prior to fear extinction (15 CS, Extinction 1), animals were given injections of Bexarotene (RXR agonist, 50 mg/kg) or Vehicle (DMSO) (Figure 5N). No differences between groups were detected. Twenty-four hours later during a second extinction session (Extinction 2) animals previously treated with Bexarotene prior to Extinction 1 expressed significantly reduced fear compared with controls. These pharmacological agents predictably affected fear extinction learning in a manner consistent with our hypothesized role for the *Drd2* population being a fear supporting population whose activation or inhibition is sufficient to modulate fear. Antagonizing $G_{\alpha s}$-coupled ADORA2A dramatically decreased fear expression, as would be expected by decreasing activity of a fear-supporting population. In contrast, antagonizing $G_{\alpha i}$-coupled NPY5R increased fear expression

as would be expected by decreasing inhibition of (increasing activity of) a fear-supporting population. Activation of RXR may act to generally enhance extinction consolidation as observed with Bexarotene treatment, although the mechanism by which this may occur is unclear as RXRs are nuclear hormone receptors with a variety of binding partners[57].

Dynamic regulation of *Drd2* after fear extinction.

Drd2 expression was not significantly changed after fear conditioning in the above reported TRAP study; however, the literature suggests that D2R is involved in the control and consolidation of fear and extinction learning. Therefore, the dynamic regulation of *Drd2* was examined after fear extinction. Two groups (FC 1 and FC 30) of animals were fear conditioned (5 CS/US, 0.65 mA foot shock)(Supplemental Figure 8A). Twenty-four hours later three groups received differing CS exposures; FC30 received 30 CS presentations; FC1 received 1 CS presentation and remained in the chamber for the remainder of the session; HC30 received exposure to 30 CS presentations with no previous training experience. A home cage (HC) control group was also included. Each cohort of mice was sacrificed 2 hours following extinction training, RNA was isolated from 1 mm micropunch centered over the CeA, and *Drd2* expression levels were examined via qPCR (Supplemental Figure 8B and C). *Drd2* mRNA expression was significantly increased in the extinction group (FC30) when compared to all other groups and no significant change from HC was found in either HC30 or FC1 groups. These data suggest that dynamic regulation of *Drd2* may be involved in the consolidation of fear extinction, potentially increasing inhibition of this population through $G_{\alpha i}$ coupled D2 receptors. This dynamic regulation with fear extinction consolidation is consistent with our findings of differential modulation of extinction learning with targeted *Drd2*-cell type specific pharmacological approaches.

Discussion

The present study: 1) Examined the distribution and co-expression of *Drd2* with *Drd1a, Adora2a, Crh, Nts, Sst, Prkcd,* and *Tac2* across the A/P axis; 2) Identified *Drd2* expressing neurons as a fear supporting population through direct chemogenetic manipulation; 3) Characterized cell-type specific translational changes following fear conditioning and identified many dynamically regulated genes including *Adora2a, Npy5r, Rxrg, Sst5r, Fgf3, Erbb4, Fkbp14, Dlk1,* and *Ssh3*; and finally, 4) Pharmacologically manipulated ADORA2A, NPY5R, and RXR to assess their viability as potential *Drd2* cell-type specific targets for pharmacological enhancement of fear extinction.

The identification of a fear supporting population in the CeC is consistent with previous findings that the CeC specifically receives input from the fear promoting prelimbic cortex as well as other anxiety and pain related areas[58,59]. Our findings of strong co-expression of *Drd2* and *Adora2a* but not *Drd1a* are consistent with findings in other regions[42]. Interestingly, we found lower co-expression of *Drd2* with *Prkcd* in the posterior CeL compared to reports by De Bundel et al. and in the anterior CeC compared to reports by Kim et. al.[19,60]. The former instance is explained by De Bundel's use of a Drd2::GFP reporter mouse; reporter mice may strongly express a transgene in cells that only express lower levels of the native transcript and thus were below our detection criteria. Likewise, discrepancies with Kim et al., are likely due to our use of stricter criteria for positive expression. In either case, data from both reports support our findings of *Drd2* as a fear supporting population. Another interesting discrepancy between our data and that reported by Kim et al., is that we demonstrate very little *Drd1a* expression in the posterior

CeL. This is remarkable because the posterior CeL contains the densest *Crh, Nts, Sst, Prkcd,* and *Tac2*, populations that were reported to correspond with *Drd1a* neurons in this area. This discrepancy may again be due to our more strict criteria for positively expressing cells.

Overall, the presented behavioral data are remarkably consistent. Manipulation of the *Drd2* neuronal population either through Gs–DREADD, or the inhibition of ADORA2A ($G_{\alpha s}$) or NPY5R ($G_{\alpha i}$), drives fear expression in directions consistent with this being a fear supporting population. ADORA2a is known to be co-expressed with D2R and these receptors have been shown to have opposing actions, suggesting that both receptors may be viable candidates for modulation of a single sub-population[61,62]. An important consideration is that drugs were administered systemically, thus making it impossible to claim that effects were mediated exclusively through receptors found in the CeA. However, as the goal of this line of research is to identify potentially clinically relevant targets for enhancement of therapy, it is advantageous to test candidates as they would be used in the clinic, that is, systemically and prior to exposure therapy.

The finding of an acute increase in locomotion with global $A_{2A}R$ antagonism is consistent with reports in the literature and is expected because manipulation of the indirect pathway is a common treatment for Parkinson's Disease[27,61]. Additionally, locomotor effects observed with the ADORA2A antagonist closely mirror results observed from direct DREADD manipulation of *Adora2a* neurons[63]. The transience of locomotor effects as well as the absence of effects on anxiety-like behavior suggest that changes in freezing during subsequent testing are due to effects on learning and are not the result of locomotor changes. These results are also consistent with reports that ADORA2A antagonism with SCH58261 produces deficits in contextual fear conditioning[64].

Profiling changes in actively translating RNAs using TRAP protocols provides a unique window into the acute responses of these neurons to a learning event. We sought to identify transcripts that were differentially regulated following fear learning, so that changes in protein activity might be pharmacologically opposed at a later time point; during fear extinction. There are several other important time points to compare including prior to and following fear extinction, which will be important subjects for future investigation.

Bioinformatic analysis of TRAP-seq data emphatically confirms specificity of pull-down to amygdala neurons. Network analysis reveals that identified differentially expressed genes are primarily co-expressed. Although genes do not to a great extent belong to a single pathway, they are part of common ontologies suggesting domains of proteins that may be valuable to interrogate in the future. Several genes including *Adora2a, Sst5r, Npy5r, Fgf3* and *Erbb4,* have been directly implicated in or are in well-established signaling pathways implicated in the control of fear learning. Others genes such as *Rxrg, Gpr6, Fkbp14, Parva, Dlk1* and *Ssh3* have not been studied in the context of fear biology, but may provide valuable insights upon further investigation. Interestingly, several of these genes, most prominently *Adora2a* and *SstR5*, have been implicated in human anxiety disorders[65,66].

Data presented here identifies potential pharmacological enhancers of extinction by leveraging cell-type specific techniques in a fear-controlling population. This approach represents a potential avenue for predicting novel targets for the modulation of emotional learning, generating more specific and effective treatments of psychiatric illnesses such as PTSD.

Methods

Animals

C57BL/6J mice were obtained from Jackson Laboratories (Bar Harbor, ME). B6.FVB(Cg)-Tg(Drd2-Cre)ER43Gsat/Mmucd mice were obtained from the MMRRC and produced as part of the GENSAT BAC Transgenic Project. Rosa26 fs-TRAP (B6.129S4-Gt(ROSA)26Sortm1(CAG-EGFP/Rpl10a,-birA)Wtp/J) mice were obtained from Jackson Laboratories. *Drd2*-TRAP mice were generated by crossing *Drd2*-Cre and Rosa26 fs-TRAP lines. All mice were adult (8-12 week) at the time of behavioral training. All mice were group housed and maintained on a 12hr:12hr light:dark cycle. Mice were housed in a temperature-controlled colony and given unrestricted access to food and water. All procedures conformed to National Institutes of Health guidelines and were approved by Emory University Institutional Animal Care and use Committee. Animal numbers were calculated using G*Power 3 software using previous experiments to inform expected means and standard deviations for expected large and medium effect sizes for chemogenetic and pharmacological manipulations respectively[1]. Animals were assigned to groups based upon genotype or randomized to treatment. Experimenter was blinded to genotype of animals. Blinding to drug administration was not possible; however, animal id's were coded during data analysis.

Surgical Procedures

Mice were deeply anesthetized with a Ketamine/Dexdormitor (medetomidine) mixture and their heads fixed into a stereotaxic instrument (Kopf Instruments). Stereotaxic coordinates were identified from Paxinos and Franklin (2004) and heads were leveled using lambda and bregma. For viral delivery (Figure 3), a 10µl microsyringe (Hamilton) was lowered to coordinates just above CeA (A/P -1.2, M/L +/- 3.0, D/V -4.8) and .5 µl of AAV_5-hSyn-DIO-rM3D(Gs)-mCherry (UNC Viral Vector Core) was infused at .1µl/min using a microsyringe pump. After infusion, syringes remained in place for 15 min before being slowly withdrawn. After bilateral infusion, incisions were sutured closed using nylon monofilament (Ethicon). For all surgeries, body temperature was maintained using a heating pad. After completion of surgery, anesthesia was reversed using Antisedan (atipamezole) and mice were allowed to recover on heating pads.

Drug Administration

Clozapine-N-Oxide (Sigma) was diluted in sterile saline and administered at 1 mg/kg i.p. 30 min prior to behavioral testing. Istradefylline (Tocris # 5417) was dissolved in DMSO and diluted to 10% DMSO, 1% NP-40 in sterile saline immediately prior to i.p. administration at 3 mg/kg. Velneperit (MEdChem Exprpess #342577-38-2) has very low solubility in water, thus it was dissolved in pure DMSO prior to injection and injected at 100 mg/kg in .03 ml using an insulin syringe. Bexarotene (Tocris # 5819) also has limited solubility in water, thus it was dissolved in pure DMSO prior to injection and injected i.p. at 50 mg/kg in a volume of .03 ml using an insulin syringe. These volumes of pure DMSO have been previously tested and validated to cause no adverse health effects in adult mice.

Behavioral Assays

Auditory Cue-Dependent Fear Conditioning

Mice were habituated to fear conditioning chambers (Med Associates Inc., St Albans, VT) for 10 min each of two days prior to fear conditioning. Mice were conditioned to five tones (30s, 6 kHz, 65-70db) co-terminating with a 1 s foot shock (.65 mA, 1 mA for *Drd2* expression experiment, or .4 mA for mild conditioning).

Auditory Cue-Dependent Extinction

Cue-dependent fear extinction was tested 24 h after fear conditioning and extinction retention occurred 24 h after fear expression. For extinction, mice were placed in a novel context with a different olfactory cue, lighting and flooring and exposed to 15 or thirty 30 s, 65-70 db tones with an inter-trial-interval of 60 s. Freezing was measured using Freeze View software (Coulbourn Instruments Inc., Whitehall, PA).

Open Field

Open field chambers (Med Associates) were placed in a dimly lit room. Mice were placed in the chamber for 10 min and allowed to explore.

Brain collection following behavior for qPCR analysis of Drd2

Examination of changes in *Drd2* expression following behavioral experiments included 4 groups: 1) a Home Cage (HC) control group that remained undisturbed in their home cage throughout the experiment; 2) the primary experimental group (FC30), which received fear conditioning and extinction (30 CS) as described above; 3) a tone-alone control group (HC30) that remained in the home cage during training but was exposed to the same 30 tone presentations as the FC30 group in the extinction context; 4) a conditioned control group (FC1) that was fear conditioned as in the FC30 group but only exposed to one tone 24 h later. Brains were extracted 2 h after fear extinction or tone exposure. Brains from HC control animals were also extracted during this time.

Real Time PCR

RNA was reverse transcribed using SuperScript 4 (Invitrogen). Quantitative PCR was performed on cDNA with each sample run in triplicate technical replicates. Reactions contained 12 µl Taqman Gene Expression Master Mix (Applied Biosystems), 1 µl of forward and reverse primer, 1 µl of 5 ng/ul cDNA, and 6 µl water. Primers were proprietary FAM labeled probes from Life Technologies. Quantification of qPCR was performed on Applied Biosystems 7500 Real-Time PCR System. Cycling parameters were 10 min at 95°C, 40 cycles of amplification of 15 s at 95°C and 60 s at 60°C, and a dissociation step of 15 s 95°C, 60 s at 60°C, 15 s 95°C. Fold changes were calculated as ΔΔCT values normalized to levels of GAPDH or 18S mRNA. Values presented as fold change +/- s.e.m.

RNA-Seq Library Preparation

Libraries were generated from 1ng of Total RNA using the SMARTer HV kit (Clonetech), barcoding and sequencing primers were added using NexteraXT DNA kit. Libraries were validated by microelectrophoresis, quantified, pooled and clustered on Illumina TruSeq v3 flowcell. Clustered flowcell was sequenced on an Illumina HiSeq 1000 in 50-base paired end reactions. Approximately 25 million sequencing reads were collected per sample.

Analysis of RNA sequencing data

RNA sequencing data was analyzed using Tuxedo DESeq analysis software. Differential expression between HC and FC groups were obtained and used for further analysis. Using the q value of less than .05 as a cut-off, only highly significant returns were used for further analysis. To ensure that genes had a large enough difference in expression to warrant pharmacological manipulation, only those with differences in expression greater than $2^{.5}$ or ~141% were considered.

Bioinformatics

Enrichment analysis for Mouse Gene Atlas dataset and Jensen Compartments, was performed with Enrichr (Chen, E. Y. et al.).

Enrichment analysis for Gene Ontology Processes and Diseases was performed using MetaCore (Clarivate) Gene Set Enrichment Analysis was used to identify gene with concordant directional effects (Subramanian, A. et al.). Weighted gene network analysis was performed using GeneMania at the default setting (ref: Warde-Farley, D. et al.). Network data are presented in Dataset S3 A–C and were visualized in Cytoscape (ref: Montojo J, et al. (2010) GeneMANIA Cytoscape plugin: Fast gene function predictions on the desktop. Bioinformatics 26(22):2927–2928.) and presented in Fig. 4. Next using the MetaCore "Drugs for Drug targets" 'Drug Gene Interaction Database' (http://www.dgidb.org/) returns were examined for having a known pharmacological agent that modifies its activity. Genes lacking viable pharmacological modulators were eliminated.

Translating Ribosome Affinity Purification

TRAP procedure was completed as described in Heintz et. al., (2014)[30]. Adult *Drd2*-TRAP mice were anesthetized; their brains removed and snap frozen. Bilateral 1mm punches were collected and pooled from 3 animals per sample (n= 3 (HC) and 4 (FC)). Messenger RNA was isolated from eGFP-tagged ribosomes, as described in reference[30]. RNA was assessed for quality using the Bioanalyzer Pico (Agilent, Santa Clara, CA). All samples returned RINs (RNA Integrity Numbers) of 8.5 or greater.

Statistics

Statistical analyses were performed using Prism 6 or 7 by Graph Pad. All data presented as mean +/- s.e.m. Fear extinction experiments were examined using a repeated-measures ANOVA with drug as the between-subjects factor and tone presentation as the within subject factor. Open field activity or acoustic startle for Istrafefylline experiments was compared using a repeated measures ANOVA and a Tukey's multiple comparisons analysis. For qPCR delta delta CT's of data were compared by Student's t-test between bound and unbound fractions. For all tests statistical significance was set at $p < .05$. For quantification of FISH RNA-Scope results, numbers of expressing verses co-expressing cells were compared using Mann-Whitney's test.

FISH - RNA Scope Staining

Staining for RNA of interest was accomplished using RNA Scope Fluorescent Multiplex 2.5 labeling kit. Probes utilized for staining are: mm-Nts-C1, mmNts-C2, mm-Tac2-C2, mm-Sst-C1, mm-Sst-C2, mm-Crh-C1, mm, Prkcd-C1, mm-Prkcd-C3, mm-Drd2-C3, mm-Dkk3-C1, mm-Drd1a-C2, mm-Adora2a-C1. Brains were extracted and snap-frozen in methyl-butane on dry ice. Sections were taken at a width of 16 µm. Procedure was completed to manufacturers specifications.

Image acquisition

Images were acquired with the experimenter blinded to the probes used. 16-bit images of staining were acquired on a Leica SP8 confocal microscope using a 10x, 20x, or 40x objective. Images for 1A-F and 4B and E were acquired using a Zeiss Imager a1 with a 2x or 4x objective. Within a sample, images used for quantification were acquired with identical settings for laser

power, detector gain, and amplifier offset. Images were acquired as a z-stack of 10 steps of .5 µm each. Max intensity projections were then created and analyzed.

Figure Legends

Figure 1. Comparison of CeA *Drd2, Drd1a,* and *Adora2a* populations.

Expression of *Dkk3, Drd2, Drd1a,* and *Adora2a* were examined with FISH (RNA Scope, ACD Biosystems)**. A.** Schematic of amygdala compartments within the temporal lobe. **B.** DAPI (Grey). **C.** *Dkk3* (Green) is expressed in a population of BLA pyramidal neurons. **D.** *Drd1a* (Red) is expressed in striatum, weakly in some BLA cells, ITC's (especially Im), strongly in CeL and CeM, but weakly in the CeC. **E**. *Drd2* (Cyan) is expressed in striatum, CeC, CeL, but weakly in the CeM and not ITCs or BLA. **F.** Overlay of B-E. The dorsal CeA especially CeL expresses both *Drd2* and *Drd1a* populations; however theses populations segregate primarily to the CeC and CeM , respectively, more ventrally **G.** Schematic of higher magnification anterior dorsal region of CeA. **H.** DAPI (Grey). **I.** *Adora2a* (Green) is expressed strongly CeC, CeL and dorsal CeM. **J.** *Drd1a* (Red) is expressed strongly in CeL and CeM, but little expression is found in CeC. **K.** *Drd2* (Cyan) is expressed strongly in CeC, CeL and dorsal CeM. **L.** Overlay of H-K. *Adora2a* and *Drd2* entirely co-express. Very few examples of co-expression between *Drd1a* and either *Drd2* or *Adora2a* are found. Scale Bar: A-F 500 um, G-L 50 uM.

Figure 2. Co-localization of Drd2 with *Crh, Nts, Prkcd, Sst,* and *Tac2.*

Drd2 does not strongly co-express with any markers examined in anterior CeA. *Drd2* moderately co-expresses with *Prkcd* in posterior CeC and CeL. **A.** Density of *Drd2* cell population across anterior and posterior CeA represented as a percentage of total DAPI labeled cells. The strongest *Drd2* expression is found in anterior CeC and CeL. **B.** Quantification of *Drd2* co-expression with different CeA markers at anterior and posterior positions as a percentage of total *Drd2* expressing cells (CeC: 2-way ANOVA with anterior vs. posterior set as row factor ($F(1,79)=13.2$), $p=.0005$) and individual RNAs set as column factor ($F(4,79)=16.19$, $p<.0001$). Interaction ($F(4,79)=10.56$, $p<.0001$) and Sidaks multiple comparisons test within row: posterior: Crh vs. Prkcd $p < .0001$, Nts vs. Prkcd $p < .0001$, Sst vs. Prkcd $p< .0001$, and Tac2 vs. Prkcd $p < .0001$; CeL 2-way ANOVA with anterior vs. posterior set as row factor ($F(1,74)=2.817$), $p=.0975$) and individual RNAs set as column factor ($F(4,74)=5.288$, $p<.0008$). Interaction ($F(4,74)=3.901$, $p<.0063$) and Sidaks multiple comparisons test within row: anterior: Crh vs. Sst $p < .05$, posterior: Nts vs. Prkcd $p< .005$, Sst vs. Prkcd $p < .0005$, Tac2 vs. Prkcd $p < .05$; CeM: 2-way ANOVA with anterior vs. posterior set as row factor ($F(1,77)=3.024$), $p = .086$) and individual RNAs set as column factor ($F(4,77)=2.578$, $p<.05$). Interaction ($F(4,77)=1.456$, $p = .22$) and Sidaks multiple comparisons test within row: Posterior: Crh vs. Tac2 $p < .04$, Tac2 vs. Prkcd $p < .005$, Tac2 vs Sst $p < .01$). **C-F.** Map of CeA at A/P: -.94, -1.22, -1.46, and -1.58 respectively. **G-J.** DAPI (Grey) expression in at A/P: -.94, -1.22, -1.46, and -1.58 respectively. **K.** *Crh* (Green)is found primarily in CeL at A/P: -.84. **L.** *Prkcd* (Green)is found in a isolated population at the ventral aspect of the CeC at A/P -1.22. **M.** *Prkcd* (Green) is densely expressed in CeC and CeL at A/P: -1.46. **N.** *Sst* (Green) is densely expressed in CeL and more diffusely in CeM at A/P: -1.58. **O.** (Red) *Tac2* is expressed in ventral CeC and CeM at A/P: -.94. **P.** *Nts* (Red) is expressed almost exclusively in CeM at A/P: -1.22. **Q.** *Nts* (Red)is expressed densely in CeL and diffusely in CeM at A/P: -1.46. **R.** *Crh* (Red) is expressed densely in CeL and more diffusely in CeM at A/P: -1.58. **S.** *Drd2* (Cyan) is expressed strongly in CeC and CeL and more

weakly in CeM at A/P: -.82. **T.** *Drd2* (Cyan) is expressed strongly in CeC and CeL and more weakly in CeM at A/P: -.94. **U-V.** *Drd2* (Cyan) is expressed more diffusely throughout CeA at A/P -1.46 and -1.58 respectively. **W-Z.** Overlay of G-V. Scale Bar: A-Z 100um.

Figure 3. Cell-type specific manipulation of and TRAP isolation from CeA *Drd2* population.

A. Schematic of experimental design. **B.** Representative expression pattern of mCherry-tag expression in *Drd2* neurons of the amygdala. Scale Bar: 200 um. **C.** Collapsed over-lay of expression pattern of mCherry for Cre-expressing experimental animals. Expression is generally constrained to CeC and CeL with limited expression in CeM. **D.** Mice were weakly fear conditioned to 5 CS/US pairings (6 kHz tone, .4 mA foo-shock) (2-way RM ANOVA $F(1,18)= 4.382$, $p > .05$). Mice were injected i.p. with CNO 30min prior to fear extinction session. Mice expressing Gs-DREADD-mCherry expressed significantly more fear during the entire extinction session than non-carrier controls (2-way RM ANOVA $F(1,18)=11.49$, ** $p < .01$). Twenty-four hours later during the second extinction (retention) session mice expressing Gs-DREADD-mCherry expressed significantly more fear (2-way RM ANOVA $F(1,18)=7.512$, * $p < .05$). **E.** Schematic of TRAP experiment. Animals were fear conditioned (5 CS/US, .65 mA foot-shock) or exposed to training environment. 2 hours later animals were sacrificed, 1 mm punches centered over CeA were taken and TRAP procedure was completed. **F.** Selected differential expression results of fear conditioned vs. control animals with log-fold change on x-axis. Genes found to be down-regulated following fear conditioning compared to controls (Blue, Leftward) include *Erbb4, Dlk1, Parva, Ssh3, Ttr,* and *Kcnj13*. Genes found to be up-regulated following fear conditioning compared to controls (Red, Rightward) include *Adora2a, Gpr6, Ppp1cc, Rxrg, Fgf3, Npy5r, Sstr5, Fkbp14* and *Gprin3*.

Figure 4. Bioinformatic analysis of differentially expressed genes in *Drd2* population following fear conditioning.

A. Enrichment analysis for the MetaCore Gene Ontology Processes identifies highly significant processes related to gene changes in *Drd2* neurons. **B.** Enrichment analysis for the MetaCore Gene Ontology Diseases identifies highly significant diseases related to gene changes in *Drd2* neurons. **C.** Weighted Network of genetically annotated transcripts showing differential gene expression. Differentially expressed transcripts were analyzed with the GeneMania Cytoscape plug-in using the default setting, but without extending the network with additional nodes. Genes that were not connected with others are not represented. The node size represents the -log(FDR-adjusted P-value), while the intensity of the color represents logFC (red nodes denote up-regulation in FC, while blue nodes denote down-regulation). The between-nodes edges represent relationships, the color of the edges represent the type of the relationship (76.5% coexpression in purple, 22% physical interactions in pink, 1.5% common pathway interactions in light blue), and the thickness of the edges denotes weight (i.e., strength of the pairwise relationship).

Figure 5. Pharmacological manipulation of ADORA2A, NPY5R, and RXR during behavior.

Adora2a, Npy5r, and *Rxrg* were found to be increased following fear conditioning; therefore, the effect of pharmacological manipulation of ADORA2A, NPY5R, and RXR during fear extinction was examined to assess their utility as potential enhancers of exposure therapy. **A.** List of pharmacological agents used, their targets and the effects of binding to target. **B.** Schematic of experimental design for examination of ADORA2A antagonism by Istradefylline prior to or following fear extinction. **C.** Three groups of animals were fear conditioned (5 CS/US, .65 mA

foot-shock). **D.** Pre-extinction injection of istradefylline (Istra/Veh group) causes significant decrease in freezing compared to vehicle injected controls (2-way RM ANOVA $F(2,71)=10.26$, $p < .0001$; Tukey's Multiple Comparisons: I/V vs. V/I $p = .0005$, I/V vs. V/V $p = .0017$, V/I vs. V/V $p = .517$). Animals that previously received istradefylline prior to fear extinction (Istra/Veh) continue to express less freezing 24-hours later during second extinction session (retention) compared to vehicle controls (Veh/Veh) and those that received istradefylline following extinction (Veh/Istra) (2-way RM ANOVA $F(2,69)= 5.381$ (2 animals removed b/c injuries from fighting, 1 from V/V and 1 from I/V), $p < .01$; Tukey's Multiple Comparisons: I/V vs. V/I $p = .0236$, I/V vs. V/V $p = .0181$, V/I vs. V/V $p = .8988$). **E.** Schematic of experimental design for examination of the effect of ADORA2A antagonism following fear conditioning. **F.** Two groups of mice were fear conditioned (5 CS/US, .65 mA foot-shock). **G.** No effect of prior istrafedylline treatment following fear conditioning was detected during first (2-way RM ANOVA $F(1,10)=1.22$, $p>.05$) or second extinction session (2-way RM ANOVA $F(1,10)=0.88$, $p>.05$). **H.** Schematic for experimental design of examination of effect of istradefylline on locomotion, center-time and acoustic startle. **I.** Pre-session administration of vehicle (Veh) or istradefylline (Istra). Day 2 istradefylline treatment caused acute increase in distance traveled compared to day 1 Vehicle that returned to baseline on day 3 Vehicle test (RM ANOVA $F(1.443,8.656)=60.77$ $p < .0001$; Tukey's Multiple Comparisons: Veh (D1) vs Istra $p=.0009$, Veh (D1) vs. Veh (D3) $p= .0984$, Veh (D3) vs. Istra $p < .0001$). **J.** Pre-session administration of vehicle (Veh) or isradefylline (Istra). Day 2 istradefylline treatment did not cause changes in anxiety like behavior (time in center). Day 3 Veh did have reduced time in center compared to Day 2 Istra; however, this is likely due to habituation (RM ANOVA $F(1.542, 9.253)=6.602$ $p < .05$; Tukey's Multiple Comparisons Test Veh (D1) vs Istra $p=.4570$, Veh (D1) vs. Veh (D3) $p= .0577$, Veh (D3) vs. Istra $p=.0440$). **K.** Pre-session administration of vehicle (Veh) or isradefylline (Istra). Day 2 treatment with istradefylline caused a decreased acoustic startle amplitude that did not persist into Day 3 vehicle treatment (RM ANOVA $F(1.794,16.14)=8.203$ $p = .0043$; Tukey's Multiple Comparisons Test Veh (D1) vs Istra $p=.0205$, Veh (D1) vs. Veh (D3) $p= .7924$, Veh (D3) vs. Istra $p=.0111$)). **L.** Schematic for experimental design of examination of effects of venelperit and bexarotene. **M.** Cohorts of mice were fear conditioned (5 CS/US, .65 mA foot-shock), no differences between groups was detected. Pre-extinction injection of velneperit caused increased freezing when compared to control vehicle group, Extinction 1 (2-way RM ANOVA, $F(1,13)=15.74$, $p < .005$). No difference between groups was detected 24-hours later during second extinction session, Extinction 2. **N.** Cohorts of mice were fear conditioned (5 CS/US, .65 mA foot-shock), no differences between groups was detected. Pre-extinction injection of bexarotene causes no within session change in behavior, Extinction 1. Twenty-four hours later during Extinction 2, animals that had previously been injected with bexarotene prior to Extinction 1 expressed significantly less freezing than vehicle injected controls (2-way RM ANOVA, $F(1,29)=5.761$, $p < .05$).

Supplemental Figure 1. Distribution of *Drd2, Adora2,* and *Drd1a* across A/P axis of CeA

The *Drd2/Adora2a* population is heavily represented in anterior CeC and CeL, while *Drd1a* is strongly represented in anterior CeL and CeM. Neither population is found at high levels in posterior CeA. **A-D.** Map of CeA at A/P: -.82, -1.0, -1.2, and -1.6 respectively. **E-H.** DAPI (Grey) expression at A/P: -.82, -1.0, -1.2, and -1.6. **I-L.** *Adora2a* (Green)expression at A/P: -.82, -1.0, -1.2, and -1.6. *Adora2a* is strongly expressed in anterior CeC and CeL (-8.2 to -1.2) but not in posterior CeA (-1.6). **M-P.** *Drd1a* (Red)expression at A/P: -.82, -1.0, -1.2, and -1.6. *Drd1a* is strongly expressed in anterior CeL and CeM (-8.2 to -1.2) but not in posterior CeA (-1.6). **Q-T.** *Drd2* (Cyan) expression at A/P: -.82, -1.0, -1.2, and -1.6. *Drd2* is strongly expressed in anterior

CeC and CeL (-8.2 to -1.2) but not in posterior CeA (-1.6). **U-X.** Merge of channels. *Drd2* and *Adora2a* form a single co-expressing population found primarily in anterior CeC and CeL that does not co-express with *Drd1a*, which is found primarily in anterior CeL and CeM. Scale Bar: A-X 200 um.

Supplemental Figure 2. Quantification of Co-expression of *Drd2* with *Prkcd, Tac2, Sst, Crh,* and *Nts* in anterior and posterior CeA.

Drd2 co-expression was quantified and represented as total number of cells expressing *Drd2*, expressing other RNA of interest, or co-expressing the two RNA's. In all cases Mann-Whitney test was performed to determine whether the co-expressing population was significantly different from each single expressing population. * p<.05. **A.** In all regions of anterior CeA very little co-expression between *Drd2* and *Prkcd* was found. **B.** Moderate co-expressoin between *Drd2* and *Prkcd* was found in posterior CeC and CeL. **C-J.** Very limited co-expression was detected between *Drd2* and *Tac2, Sst, Crh,* and *Nts,* and in all cases the *Drd2* labeled population is significantly different from the co-labeled population.

Supplemental Figure 3. Drd2-TRAP transgene expression closely recapitulates Drd2expression pattern observed with FISH. A. L10a-GFP ribosomal subunit (Green) is expressed is pattern very similar to that observed with FISH.

Supplemental Figure 4. Fear conditioning of mice for TRAP collection. Mice express significantly more freezing after fear conditioning. (Unpaired t-Test, freezing to tone vs. CS1, * p < .05).

Supplemental Figure 5. Validation of TRAP pull-down. A. Ribosomal subunit 18S is found at significantly higher levels in bound fraction, verifying ribosomal pull down (Paired t-Test, * p < .05). **B.** The ratio of *Drd2:Drd1a* is significantly higher in bound fraction vs. unbound fraction, verifying RNAs were successfully isolated from *Drd2* neurons (Paired t-Test, * p < .05).

Supplemental Figure 6. Gene set enrichment analysis.

Using the entire expression dataset in default setting genes identified in *Drd2*-TRAP fear conditioning study and humanized model of 22q11.2 deletion are significantly and concordantly regulated in inverse direction in both **A.** Prefrontal cortex and **B.** Hippocampus.

Supplemental Figure 7. Fear conditioning for Veleneperet and Bexarotene experiments. In each case two groups of animals were fear conditioned (5 CS/US, .65 mA). **A.** Animals later given Velenperit were fear conditioned. No significant differences between groups were detected(2-way RM ANOVA, $F(1,13)=.3773$, $p > .05$). **B.** Animals later given Bexarotene were fear conditioned. No significant differences between groups were detected(2-way RM ANOVA, $F(1,30)=.712$, $p > .05$).

Supplemental Figure 8. Examination of *Drd2* expression following fear conditioning and extinction.

A. Two groups of animals (FC1 and FC 30) were fear conditioned (5 CS/US, .65 mA US). **B.** Twenty-four hours three groups of animals were exposed to extinction context. FC1 was exposed to a single CS in extinction context. Percent freezing indicates freezing during tone

during CS 1 and freezing during the corresponding time when tone was played for other groups for CS 2-30, freezing during CS 1 was significantly greater than control (unpaired t-Test $F(1,12)=5.929$, $p < .0001$). HC 30 group did not receive fear conditioning, but was exposed to 30 CS's in extinction context. FC 30 was exposed to 30 CS's in extinction context and expressed more freezing than HC 30 group (Each bin examined by students t-test $p < .05$). **C.** Four groups were sacrificed 2 hours following behavior and qPCR performed on amygdala punches. FC30 group had significantly increased *Drd2*expression compared to all other groups.

Supplemental Table 1. Complete list of differentially regulated RNA's.
A. LogFC indicates log fold change between FC and Control group. Negative LogFC's indicate decreased expression compared to control while positive values indicate increased expression. FDR indicates false discovery rate corrected across multiple tests. Only $q< .05$ values are featured.

Supplemental Table 2.
Using Mouse Gene Atlas dataset, Enrichr confirms amygdala specificity of pull-down and gene change.

Supplemental Table 3. Jensen COMPARTMENTS analysis.
Jensen COMPARTMENTS analysis data set, using sequence based prediction methods confirms neuronal specificity of pull-down and gene change.

Supplemental Table 4. Drug-Gene analysis of differentially expressed genes.
Metacore 'Drug for Drug database' identifies drugs that target protein products of differentially expressed genes.

References

1 Davis, M., Walker, D. L. & Myers, K. M. Role of the amygdala in fear extinction measured with potentiated startle. *Annals of the New York Academy of Sciences* **985**, 218-232 (2003).

2 Pare, D., Quirk, G. J. & Ledoux, J. E. New vistas on amygdala networks in conditioned fear. *Journal of neurophysiology* **92**, 1-9, doi:10.1152/jn.00153.2004 (2004).

3 McDonald, A. J. Cytoarchitecture of the central amygdaloid nucleus of the rat. *The Journal of comparative neurology* **208**, 401-418, doi:10.1002/cne.902080409 (1982).

4 Hitchcock, J. M., Sananes, C. B. & Davis, M. Sensitization of the startle reflex by footshock: blockade by lesions of the central nucleus of the amygdala or its efferent pathway to the brainstem. *Behavioral neuroscience* **103**, 509-518 (1989).

5 Ciocchi, S. *et al.* Encoding of conditioned fear in central amygdala inhibitory circuits. *Nature* **468**, 277-282, doi:10.1038/nature09559 (2010).

6 McCullough, K. M., Morrison, F. G. & Ressler, K. J. Bridging the Gap: Towards a cell-type specific understanding of neural circuits underlying fear behaviors. *Neurobiol Learn Mem* **135**, 27-39, doi:10.1016/j.nlm.2016.07.025 (2016).

7 Haubensak, W. *et al.* Genetic dissection of an amygdala microcircuit that gates conditioned fear. *Nature* **468**, 270-276, doi:10.1038/nature09553 (2010).

8 Andero, R., Dias, B. G. & Ressler, K. J. A Role for Tac2, NkB, and Nk3 Receptor in Normal and Dysregulated Fear Memory Consolidation. *Neuron*, doi:10.1016/j.neuron.2014.05.028 (2014).

9 Li, H. *et al.* Experience-dependent modification of a central amygdala fear circuit. *Nat Neurosci* **16**, 332-339, doi:http://www.nature.com/neuro/journal/v16/n3/abs/nn.3322.html - supplementary-information (2013).

10 McCall, J. G. *et al.* CRH Engagement of the Locus Coeruleus Noradrenergic System Mediates Stress-Induced Anxiety. *Neuron* **87**, 605-620, doi:10.1016/j.neuron.2015.07.002 (2015).

11 Myers, K. M. & Davis, M. Mechanisms of fear extinction. *Mol Psychiatry* **12**, 120-150, doi:10.1038/sj.mp.4001939 (2007).

12 Maren, S. & Fanselow, M. S. The amygdala and fear conditioning: has the nut been cracked? *Neuron* **16**, 237-240 (1996).

13 Maren, S. & Holmes, A. Stress and Fear Extinction. *Neuropsychopharmacology : official publication of the American College of Neuropsychopharmacology* **41**, 58-79, doi:10.1038/npp.2015.180 (2016).

14 Rothbaum, B. O. *et al.* A randomized, double-blind evaluation of D-cycloserine or alprazolam combined with virtual reality exposure therapy for posttraumatic stress disorder in Iraq and Afghanistan War veterans. *The American journal of psychiatry* **171**, 640-648, doi:10.1176/appi.ajp.2014.13121625 (2014).

15 McDonald, A. J. Is there an amygdala and how far does it extend? An anatomical perspective. *Annals of the New York Academy of Sciences* **985**, 1-21 (2003).

16 Smith, Y., Bevan, M. D., Shink, E. & Bolam, J. P. Microcircuitry of the direct and indirect pathways of the basal ganglia. *Neuroscience* **86**, 353-387 (1998).

17 Pollack, A. E. Anatomy, physiology, and pharmacology of the basal ganglia. *Neurologic clinics* **19**, 523-534, v (2001).

18 Fadok, J. P. *et al.* A competitive inhibitory circuit for selection of active and passive fear responses. *Nature* **542**, 96-100, doi:10.1038/nature21047 (2017).

19 Kim, J., Zhang, X., Muralidhar, S., LeBlanc, S. A. & Tonegawa, S. Basolateral to Central Amygdala Neural Circuits for Appetitive Behaviors. *Neuron* **93**, 1464-1479.e1465, doi:10.1016/j.neuron.2017.02.034 (2017).

20 Han, S., Soleiman, Matthew T., Soden, Marta E., Zweifel, Larry S. & Palmiter, Richard D. Elucidating an Affective Pain Circuit that Creates a Threat Memory. *Cell* **162**, 363-374, doi:https://doi.org/10.1016/j.cell.2015.05.057 (2015).

21 de la Mora, M. P., Gallegos-Cari, A., Arizmendi-Garcia, Y., Marcellino, D. & Fuxe, K. Role of dopamine receptor mechanisms in the amygdaloid modulation of fear and anxiety: Structural and functional analysis. *Progress in neurobiology* **90**, 198-216, doi:10.1016/j.pneurobio.2009.10.010 (2010).

22 Abraham, A. D., Neve, K. A. & Lattal, K. M. Dopamine and extinction: a convergence of theory with fear and reward circuitry. *Neurobiology of learning and memory* **108**, 65-77, doi:10.1016/j.nlm.2013.11.007 (2014).

23 Fernandez, R. S., Boccia, M. M. & Pedreira, M. E. The fate of memory: Reconsolidation and the case of Prediction Error. *Neuroscience and biobehavioral reviews* **68**, 423-441, doi:10.1016/j.neubiorev.2016.06.004 (2016).

24 Li, L. *et al.* The Association Between Genetic Variants in the Dopaminergic System and Posttraumatic Stress Disorder: A Meta-Analysis. *Medicine* **95**, e3074, doi:10.1097/md.0000000000003074 (2016).

25 Barch, D. M., Pagliaccio, D. & Luking, K. Mechanisms Underlying Motivational Deficits in Psychopathology: Similarities and Differences in Depression and Schizophrenia. *Current topics in behavioral neurosciences* **27**, 411-449, doi:10.1007/7854_2015_376 (2016).

26 Lenka, A., Arumugham, S. S., Christopher, R. & Pal, P. K. Genetic substrates of psychosis in patients with Parkinson's disease: A critical review. *Journal of the neurological sciences* **364**, 33-41, doi:10.1016/j.jns.2016.03.005 (2016).

27 Ponnusamy, R., Nissim, H. A. & Barad, M. Systemic blockade of D2-like dopamine receptors facilitates extinction of conditioned fear in mice. *Learning & memory* **12**, 399-406, doi:10.1101/lm.96605 (2005).

28 Perez de la Mora, M. *et al.* Distribution of dopamine D(2)-like receptors in the rat amygdala and their role in the modulation of unconditioned fear and anxiety. *Neuroscience* **201**, 252-266, doi:10.1016/j.neuroscience.2011.10.045 (2012).

29 Guarraci, F. A., Frohardt, R. J., Falls, W. A. & Kapp, B. S. The effects of intra-amygdaloid infusions of a D2 dopamine receptor antagonist on Pavlovian fear conditioning. *Behavioral neuroscience* **114**, 647-651 (2000).

30 Heiman, M., Kulicke, R., Fenster, R. J., Greengard, P. & Heintz, N. Cell-Type-Specific mRNA Purification by Translating Ribosome Affinity Purification (TRAP). *Nature protocols* **9**, 1282-1291, doi:10.1038/nprot.2014.085 (2014).

31 Bourgeais, L., Gauriau, C. & Bernard, J. F. Projections from the nociceptive area of the central nucleus of the amygdala to the forebrain: a PHA-L study in the rat. *The European journal of neuroscience* **14**, 229-255 (2001).

32 Yu, K., Garcia da Silva, P., Albeanu, D. F. & Li, B. Central Amygdala Somatostatin Neurons Gate Passive and Active Defensive Behaviors. *The Journal of neuroscience : the official journal of the Society for Neuroscience* **36**, 6488-6496, doi:10.1523/jneurosci.4419-15.2016 (2016).

33 Rogan, S. C. & Roth, B. L. Remote control of neuronal signaling. *Pharmacol Rev* **63**, 291-315, doi:10.1124/pr.110.003020 (2011).

34 Wess, J., Nakajima, K. & Jain, S. Novel designer receptors to probe GPCR signaling and physiology. *Trends in pharmacological sciences* **34**, 385-392, doi:10.1016/j.tips.2013.04.006 (2013).

35 Guettier, J. M. *et al.* A chemical-genetic approach to study G protein regulation of beta cell function in vivo. *Proceedings of the National Academy of Sciences of the United States of America* **106**, 19197-19202, doi:10.1073/pnas.0906593106 (2009).

36 Alexander, G. M. *et al.* Remote control of neuronal activity in transgenic mice expressing evolved G protein-coupled receptors. *Neuron* **63**, 27-39, doi:10.1016/j.neuron.2009.06.014 (2009).

37 Gangarossa, G. *et al.* Characterization of dopamine D1 and D2 receptor-expressing neurons in the mouse hippocampus. *Hippocampus* **22**, 2199-2207, doi:10.1002/hipo.22044 (2012).

38 Gong, S. *et al.* Targeting Cre recombinase to specific neuron populations with bacterial artificial chromosome constructs. *The Journal of neuroscience : the official journal of the Society for Neuroscience* **27**, 9817-9823, doi:10.1523/jneurosci.2707-07.2007 (2007).

39 Gangarossa, G. *et al.* Spatial distribution of D1R- and D2R-expressing medium-sized spiny neurons differs along the rostro-caudal axis of the mouse dorsal striatum. *Frontiers in neural circuits* **7**, 124, doi:10.3389/fncir.2013.00124 (2013).

40 Oude Ophuis, R. J. A., Boender, A. J., van Rozen, A. J. & Adan, R. A. H. Cannabinoid, melanocortin and opioid receptor expression on DRD1 and DRD2 subpopulations in rat striatum. *Frontiers in Neuroanatomy* **8**, 14, doi:10.3389/fnana.2014.00014 (2014).

41 Le Moine, C. & Bloch, B. D1 and D2 dopamine receptor gene expression in the rat striatum: sensitive cRNA probes demonstrate prominent segregation of D1 and D2 mRNAs in distinct neuronal populations of the dorsal and ventral striatum. *The Journal of comparative neurology* **355**, 418-426, doi:10.1002/cne.903550308 (1995).

42 Oude-Ophuis, R. J., Boender, A. J., van Rozen, R. & Adan, R. A. Cannabinoid, melanocortin and opioid receptor expression on DRD1 and DRD2 subpopulations in rat striatum. *Frontiers in Neuroanatomy* **8**, doi:10.3389/fnana.2014.00014 (2014).

43 Chen, E. Y. *et al.* Enrichr: interactive and collaborative HTML5 gene list enrichment analysis tool. *BMC bioinformatics* **14**, 128, doi:10.1186/1471-2105-14-128 (2013).

44 Stark, K. L. *et al.* Altered brain microRNA biogenesis contributes to phenotypic deficits in a 22q11-deletion mouse model. *Nature genetics* **40**, 751-760, doi:10.1038/ng.138 (2008).

45 Subramanian, A. *et al.* Gene set enrichment analysis: a knowledge-based approach for interpreting genome-wide expression profiles. *Proceedings of the National Academy of Sciences of the United States of America* **102**, 15545-15550, doi:10.1073/pnas.0506580102 (2005).

46 Kramer, A., Green, J., Pollard, J., Jr. & Tugendreich, S. Causal analysis approaches in Ingenuity Pathway Analysis. *Bioinformatics (Oxford, England)* **30**, 523-530, doi:10.1093/bioinformatics/btt703 (2014).

47 Warde-Farley, D. *et al.* The GeneMANIA prediction server: biological network integration for gene prioritization and predicting gene function. *Nucleic acids research* **38**, W214-220, doi:10.1093/nar/gkq537 (2010).

48 Mouro, F. M. *et al.* Chronic and acute adenosine A2A receptor blockade prevents long-term episodic memory disruption caused by acute cannabinoid CB1 receptor activation. *Neuropharmacology* **117**, 316-327, doi:10.1016/j.neuropharm.2017.02.021 (2017).

49 Yukioka, H. [A potent and selective neuropeptide Y Y5-receptor antagonist, S-2367, as an anti-obesity agent]. *Nihon yakurigaku zasshi. Folia pharmacologica Japonica* **136**, 270-274 (2010).

50 Bhat, S. P. & Sharma, A. Current Drug Targets in Obesity Pharmacotherapy - A Review. *Current drug targets*, doi:10.2174/1389450118666170227153940 (2017).

51 Wang, S., Wen, P. & Wood, S. Effect of LXR/RXR agonism on brain and CSF Abeta40 levels in rats. *F1000Research* **5**, 138, doi:10.12688/f1000research.7868.2 (2016).

52 Jacobson, K. A. & Gao, Z. G. Adenosine receptors as therapeutic targets. *Nature reviews. Drug discovery* **5**, 247-264, doi:10.1038/nrd1983 (2006).

53 Berlacher, M., Mastouri, R., Philips, S., Skaar, T. C. & Kreutz, R. P. Common genetic polymorphisms of adenosine A2A receptor do not influence response to regadenoson. *Pharmacogenomics* **18**, 523-529, doi:10.2217/pgs-2016-0178 (2017).

54 Oertel, W. & Schulz, J. B. Current and experimental treatments of Parkinson disease: A guide for neuroscientists. *Journal of neurochemistry* **139 Suppl 1**, 325-337, doi:10.1111/jnc.13750 (2016).

55 Shimada, J. *et al.* Adenosine A2A antagonists with potent anti-cataleptic activity. *Bioorganic & Medicinal Chemistry Letters* **7**, 2349-2352, doi:http://dx.doi.org/10.1016/S0960-894X(97)00440-X (1997).

56 Shiozaki, S. *et al.* Actions of adenosine A2A receptor antagonist KW-6002 on drug-induced catalepsy and hypokinesia caused by reserpine or MPTP. *Psychopharmacology* **147**, 90-95 (1999).

57 Dawson, M. I. & Xia, Z. The Retinoid X Receptors and Their Ligands. *Biochimica et biophysica acta* **1821**, 21-56, doi:10.1016/j.bbalip.2011.09.014 (2012).

58 Missig, G. *et al.* Parabrachial nucleus (PBn) pituitary adenylate cyclase activating polypeptide (PACAP) signaling in the amygdala: implication for the sensory and behavioral effects of pain. *Neuropharmacology* **86**, 38-48, doi:10.1016/j.neuropharm.2014.06.022 (2014).

59 McDonald, A. J., Mascagni, F. & Guo, L. Projections of the medial and lateral prefrontal cortices to the amygdala: a Phaseolus vulgaris leucoagglutinin study in the rat. *Neuroscience* **71**, 55-75 (1996).

60 De Bundel, D. *et al.* Dopamine D2 receptors gate generalization of conditioned threat responses through mTORC1 signaling in the extended amygdala. *Mol Psychiatry* **21**, 1545-1553, doi:10.1038/mp.2015.210 (2016).

61 Aoyama, S., Kase, H. & Borrelli, E. Rescue of locomotor impairment in dopamine D2 receptor-deficient mice by an adenosine A2A receptor antagonist. *The Journal of neuroscience : the official journal of the Society for Neuroscience* **20**, 5848-5852 (2000).

62 Oude Ophuis, R. J. A., Boender, A. J., van Rozen, A. J. & Adan, R. A. H. Cannabinoid, melanocortin and opioid receptor expression on DRD1 and DRD2 subpopulations in rat striatum. *Front Neuroanat* **8** (2014).

63 Farrell, M. S. *et al.* A Galphas DREADD mouse for selective modulation of cAMP production in striatopallidal neurons. *Neuropsychopharmacology : official publication of the American College of Neuropsychopharmacology* **38**, 854-862, doi:10.1038/npp.2012.251 (2013).

64 Simoes, A. P. *et al.* Adenosine A2A Receptors in the Amygdala Control Synaptic Plasticity and Contextual Fear Memory. *Neuropsychopharmacology : official publication of the American College of Neuropsychopharmacology*, doi:10.1038/npp.2016.98 (2016).

65 Saus, E. *et al.* Comprehensive copy number variant (CNV) analysis of neuronal pathways genes in psychiatric disorders identifies rare variants within patients. *Journal of psychiatric research* **44**, 971-978, doi:10.1016/j.jpsychires.2010.03.007 (2010).

66 Hohoff, C. *et al.* Adenosine A(2A) receptor gene: evidence for association of risk variants with panic disorder and anxious personality. *Journal of psychiatric research* **44**, 930-937, doi:10.1016/j.jpsychires.2010.02.006 (2010).

1 Faul, F., Erdfelder, E., Lang, A.-G. & Buchner, A. G*Power 3: A flexible statistical power analysis program for the social, behavioral, and biomedical sciences. *Behavior Research Methods* **39**, 175-191, doi:10.3758/bf03193146 (2007).

Figure 1

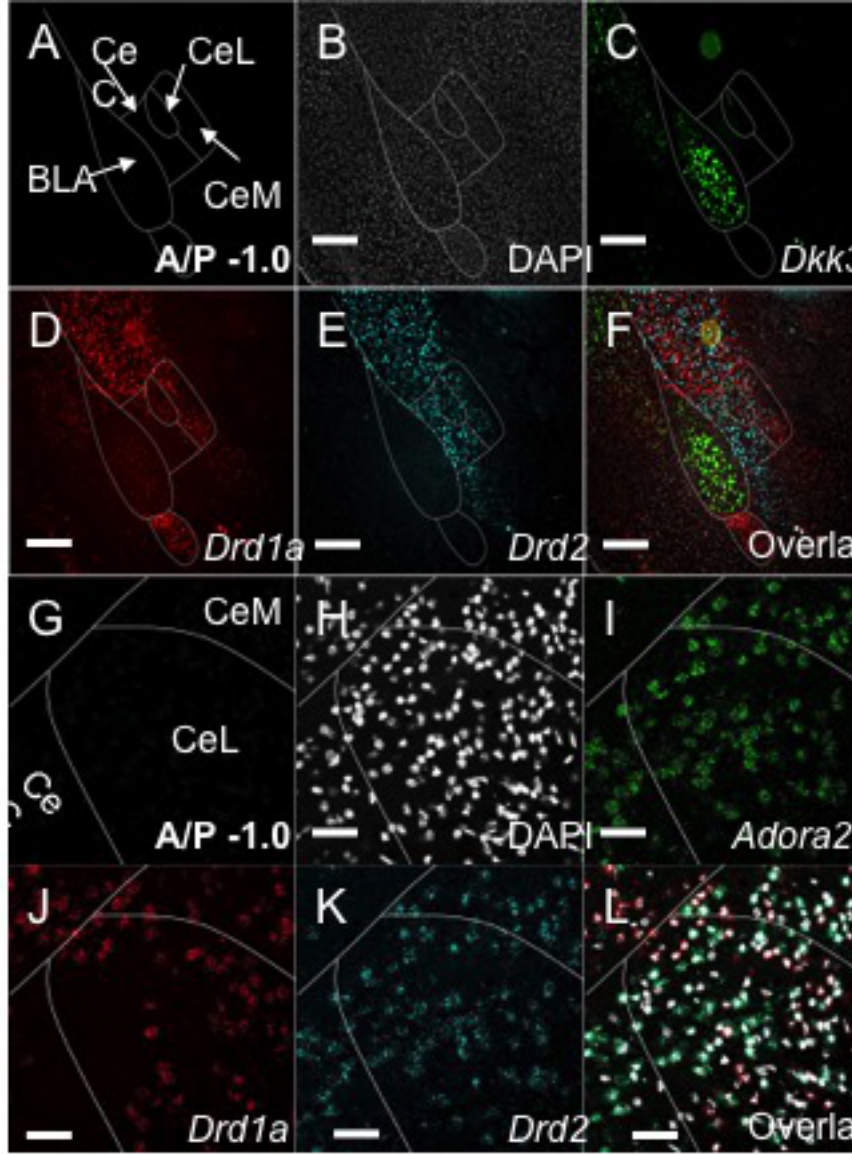
A
Ce
C
CeL
BLA
CeM
A/P -1.0
B
DAPI
C
Dkk3
D
Drd1a
E
Drd2
F
Overlay
G
CeM
CeL
Ce
A/P -1.0
H
DAPI
I
Adora2a
J
Drd1a
K
Drd2
L
Overlay

Figure 2

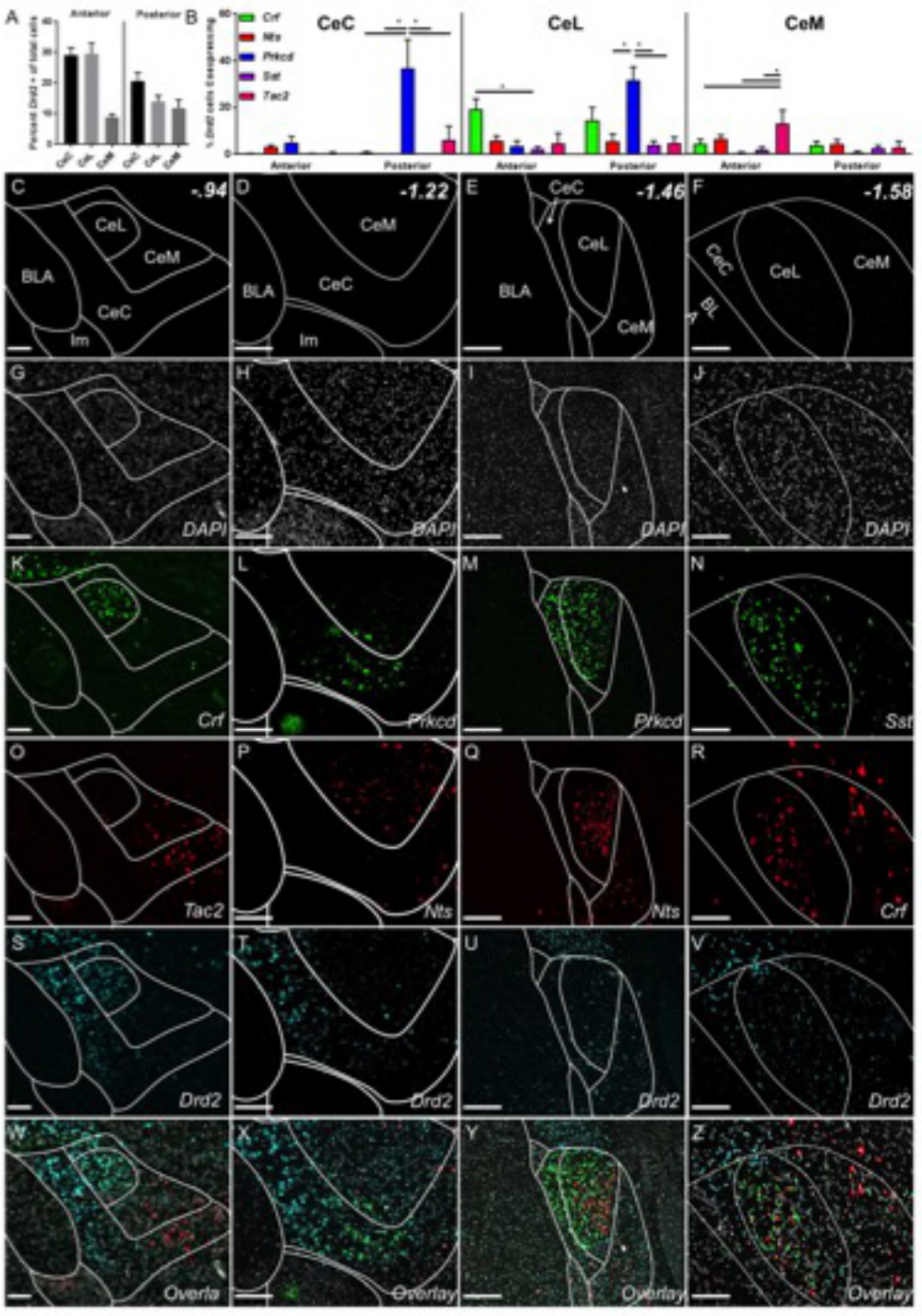
A
Anterior
Posterior
B
Crf
Nts
Prkcd
Sst
Tac2
CeC
CeL
CeM
Anterior
Posterior
C
-.94
CeL
CeM
BLA
CeC
Im
D
-1.22
CeM
BLA
CeC
Im
E
CeC
-1.46
CeL
BLA
CeM
F
-1.58
CeC
CeL
CeM
BL
G
DAPI
H
DAPI
I
DAPI
J
DAPI
K
Crf
L
Prkcd
M
Prkcd
N
Sst
O
Tac2
P
Nts
Q
Nts
R
Crf
S
Drd2
T
Drd2
U
Drd2
V
Drd2
W
Overla
X
Overlay
Y
Overlay
Z
Overlay

Figure 3

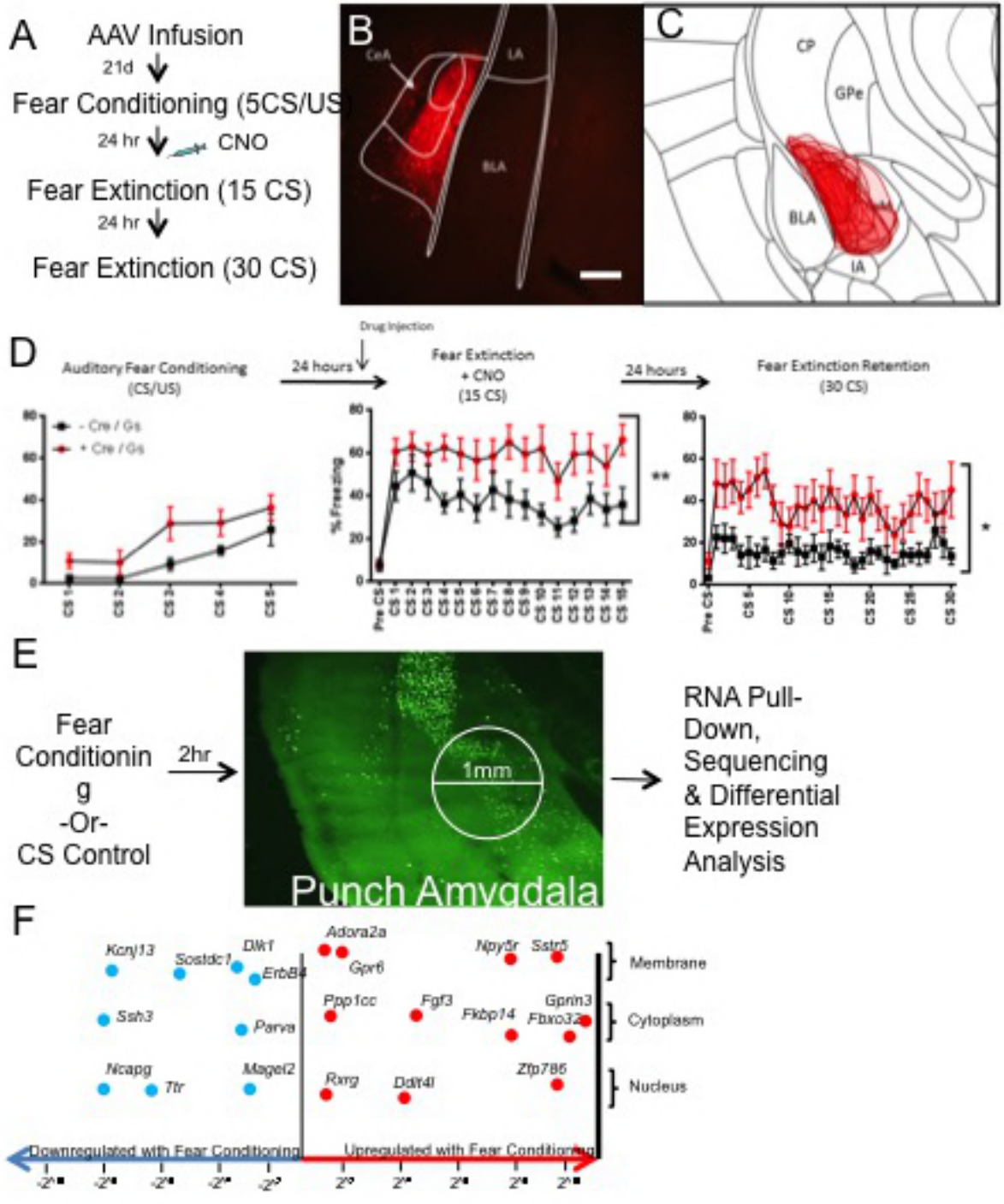
A
AAV Infusion
21d
Fear Conditioning (5CS/US)
24 hr
CNO
Fear Extinction (15 CS)
24 hr
Fear Extinction (30 CS)
B
CeA
LA
BLA
C
CP
GPe
BLA
IA
D
Auditory Fear Conditioning (CS/US)
Drug Injection
24 hours
Fear Extinction + CNO (15 CS)
24 hours
Fear Extinction Retention (30 CS)
- Cre / Gs
+ Cre / Gs
% Freezing
E
Fear Conditioning -Or- CS Control
2hr
1mm
Punch Amygdala
RNA Pull-Down, Sequencing & Differential Expression Analysis
F
Kcnj13
Sostdc1
Dkk1
ErbB4
Adora2a
Gpr6
Npy5r
Sstr5
Membrane
Ssh3
Parva
Ppp1cc
Fgf3
Fkbp14
Gprin3
Fbxo32
Cytoplasm
Ncapg
Tfr
Magel2
Rxrg
Ddit4l
Zfp786
Nucleus
Downregulated with Fear Conditioning
Upregulated with Fear Conditioning

Figure 4

A Processes

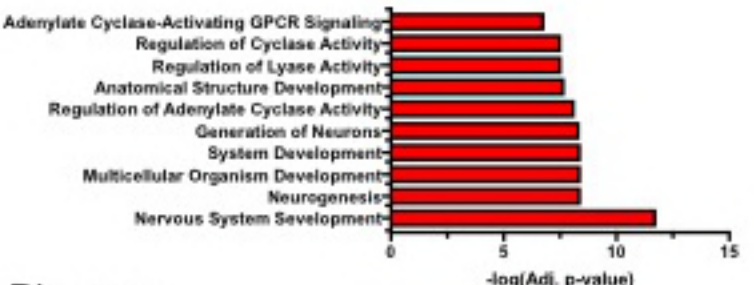

B Diseases

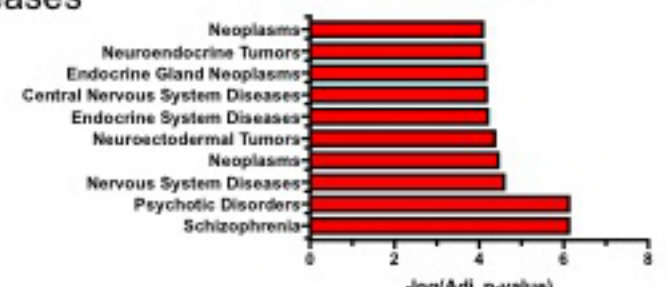

C

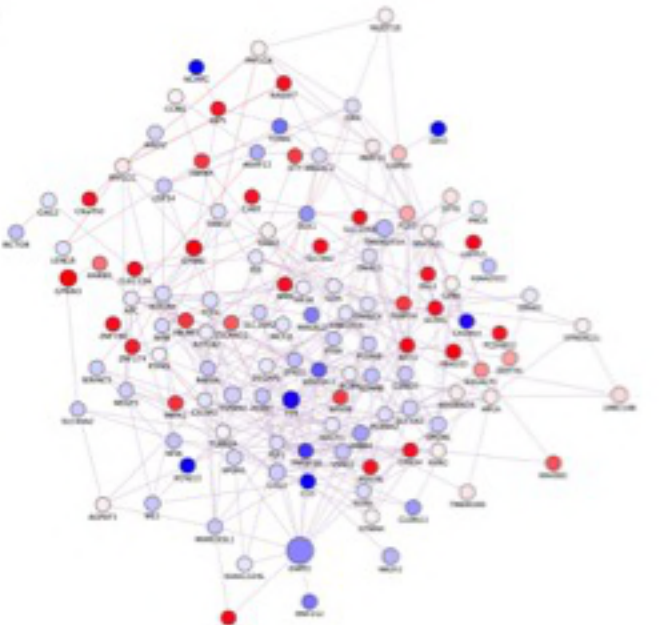

Figure 5

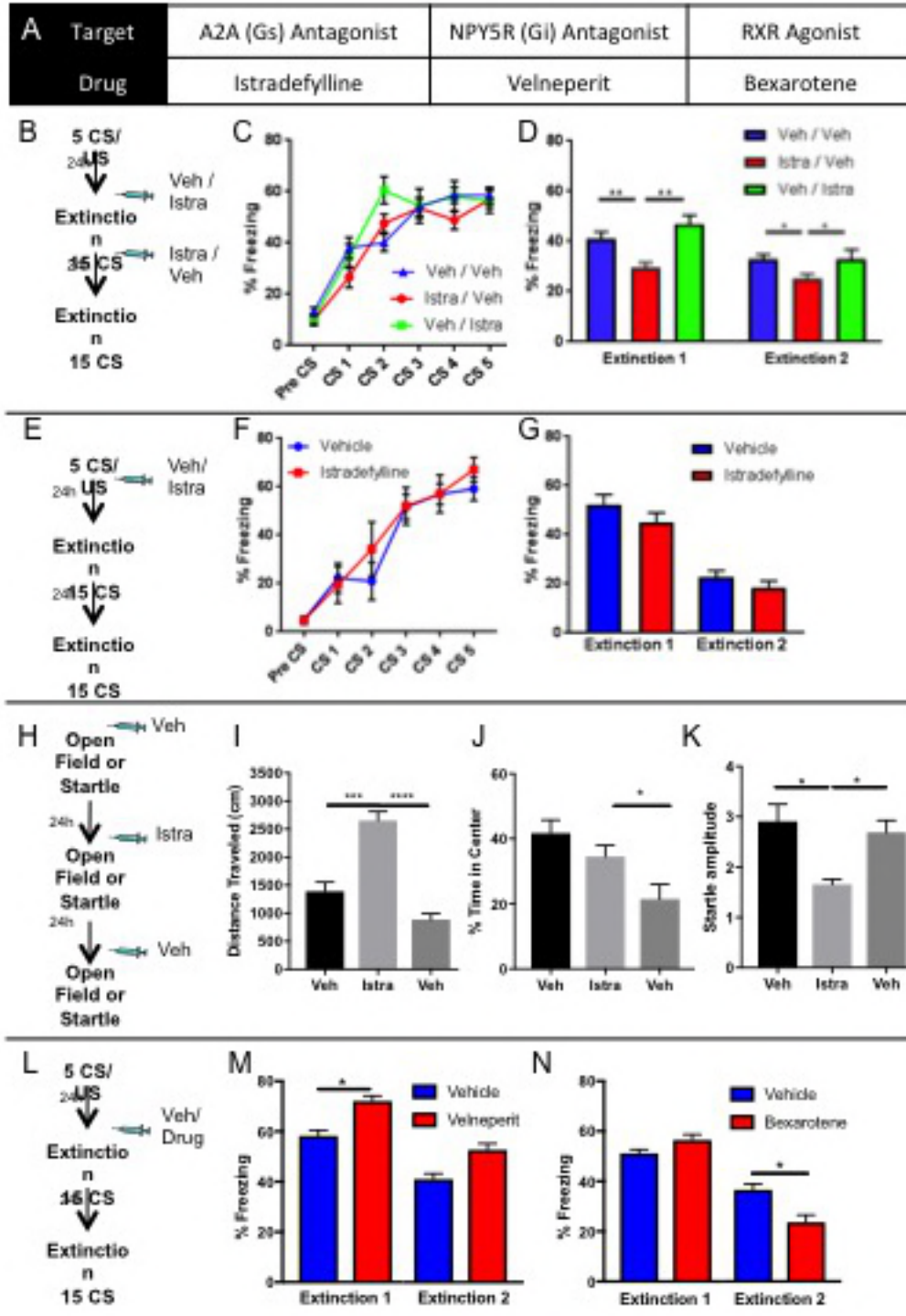
A
Target
A2A (Gs) Antagonist
NPY5R (Gi) Antagonist
RXR Agonist
Drug
Istradefylline
Velneperit
Bexarotene
B
5 CS/
24h US
Veh / Istra
Extinctio n
15 CS
Istra / Veh
Extinctio n
15 CS
C
% Freezing
Veh / Veh
Istra / Veh
Veh / Istra
Pre CS
CS 1
CS 2
CS 3
CS 4
CS 5
D
% Freezing
Veh / Veh
Istra / Veh
Veh / Istra
Extinction 1
Extinction 2
E
5 CS/
24h US
Veh/ Istra
Extinctio n
15 CS
Extinctio n
15 CS
F
Vehicle
Istradefylline
% Freezing
G
Vehicle
Istradefylline
% Freezing
Extinction 1
Extinction 2
H
Veh
Open Field or Startle
24h
Istra
Open Field or Startle
24h
Veh
Open Field or Startle
I
Distance Traveled (cm)
Veh
Istra
Veh
J
% Time in Center
Veh
Istra
Veh
K
Startle amplitude
Veh
Istra
Veh
L
5 CS/
24h US
Veh/ Drug
Extinctio n
15 CS
Extinctio n
15 CS
M
% Freezing
Vehicle
Velneperit
Extinction 1
Extinction 2
N
% Freezing
Vehicle
Bexarotene
Extinction 1
Extinction 2

S Figure 1

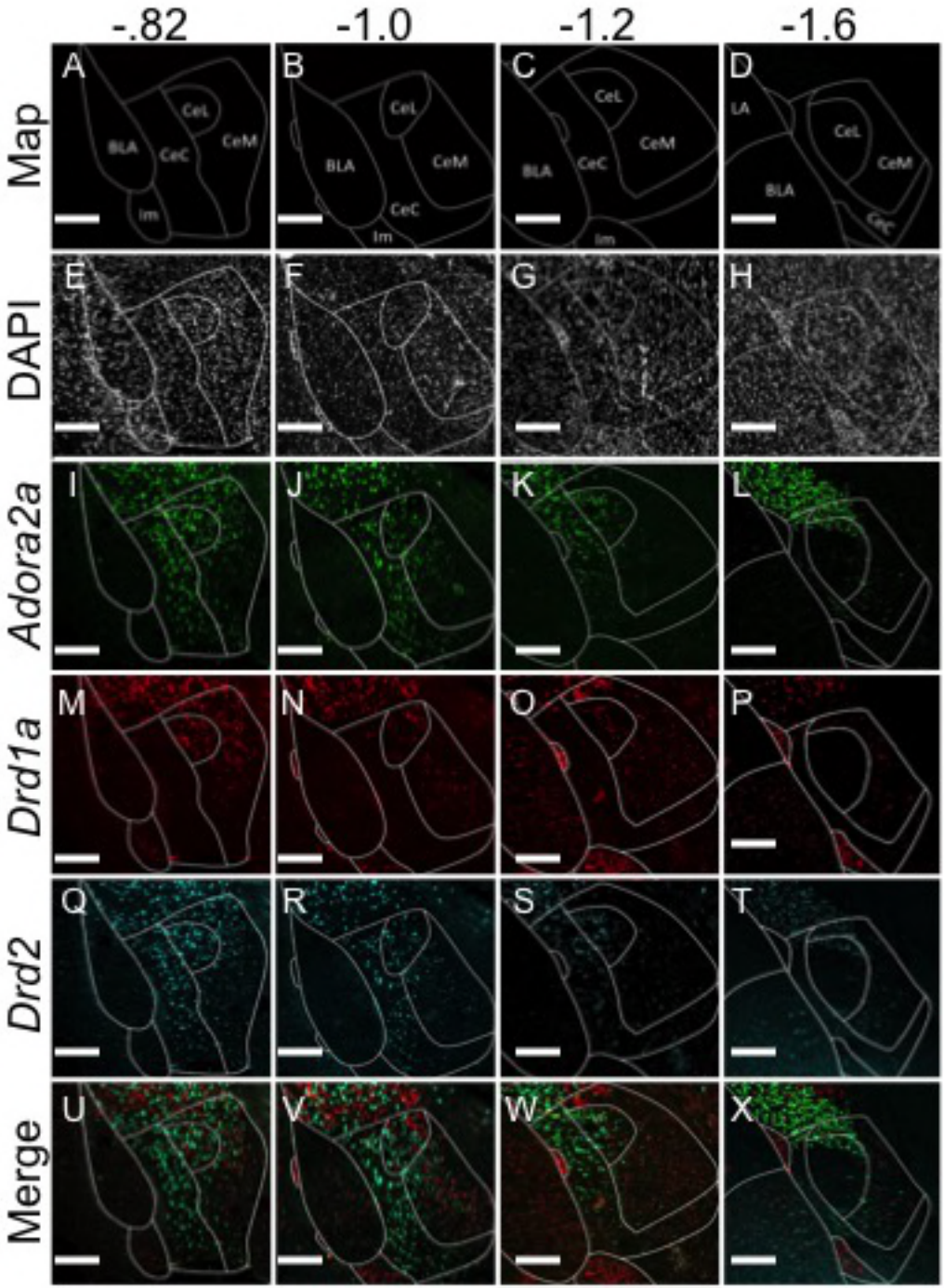
-.82
-1.0
-1.2
-1.6
Map
DAPI
Adora2a
Drd1a
Drd2
Merge
A
B
C
D
E
F
G
H
I
J
K
L
M
N
O
P
Q
R
S
T
U
V
W
X
BLA
CeC
CeL
CeM
LA
im

S Fig 2

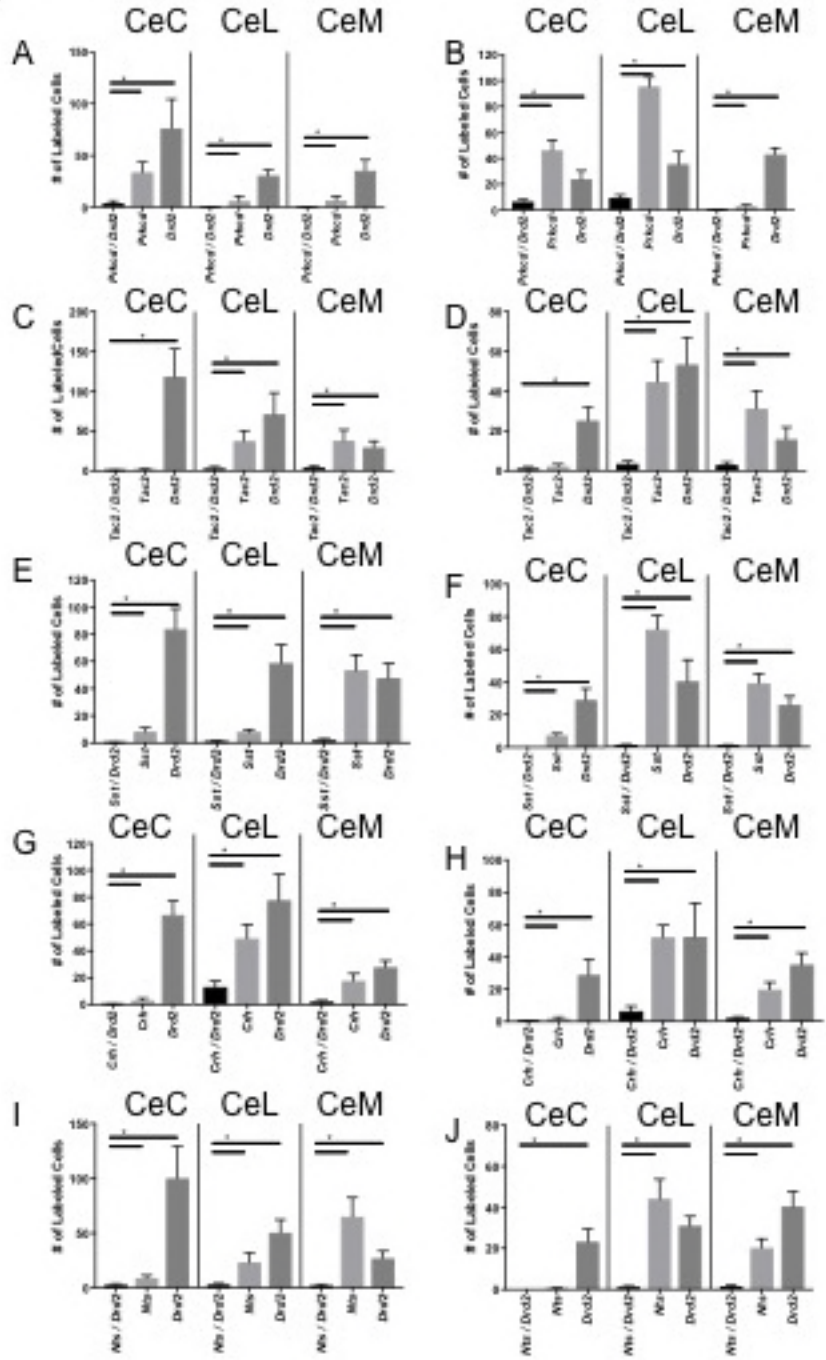
Anterior
Posterior
CeC
CeL
CeM
A
B
C
D
E
F
G
H
I
J
# of Labeled Cells

S Fig 3

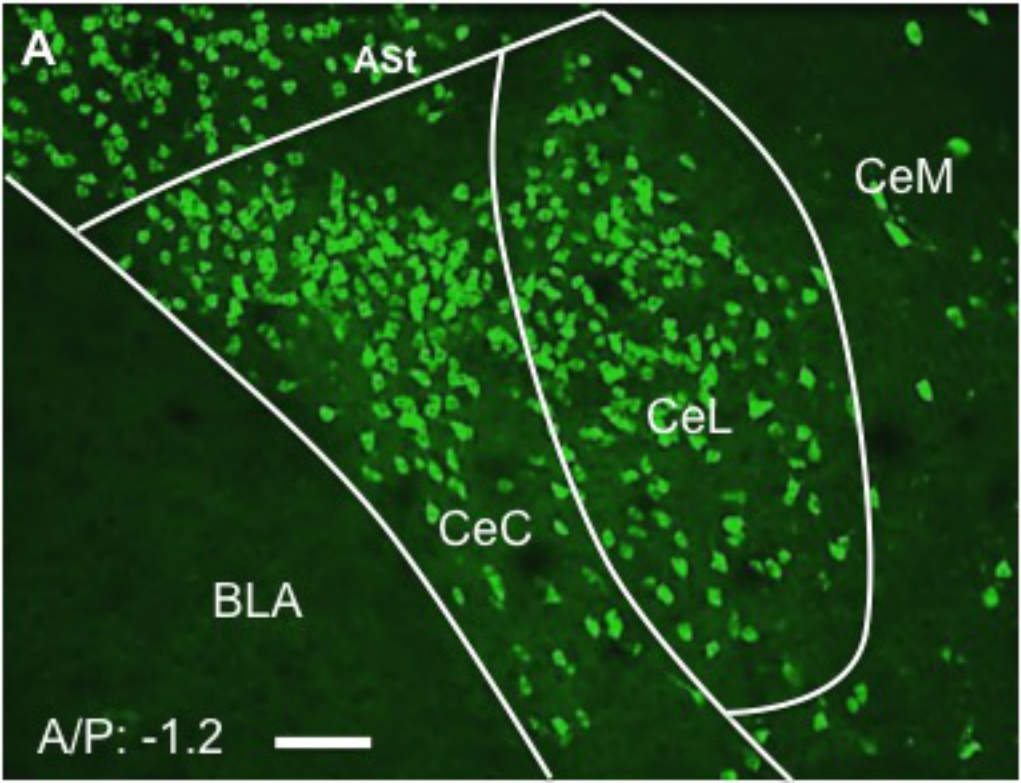

S Fig 4

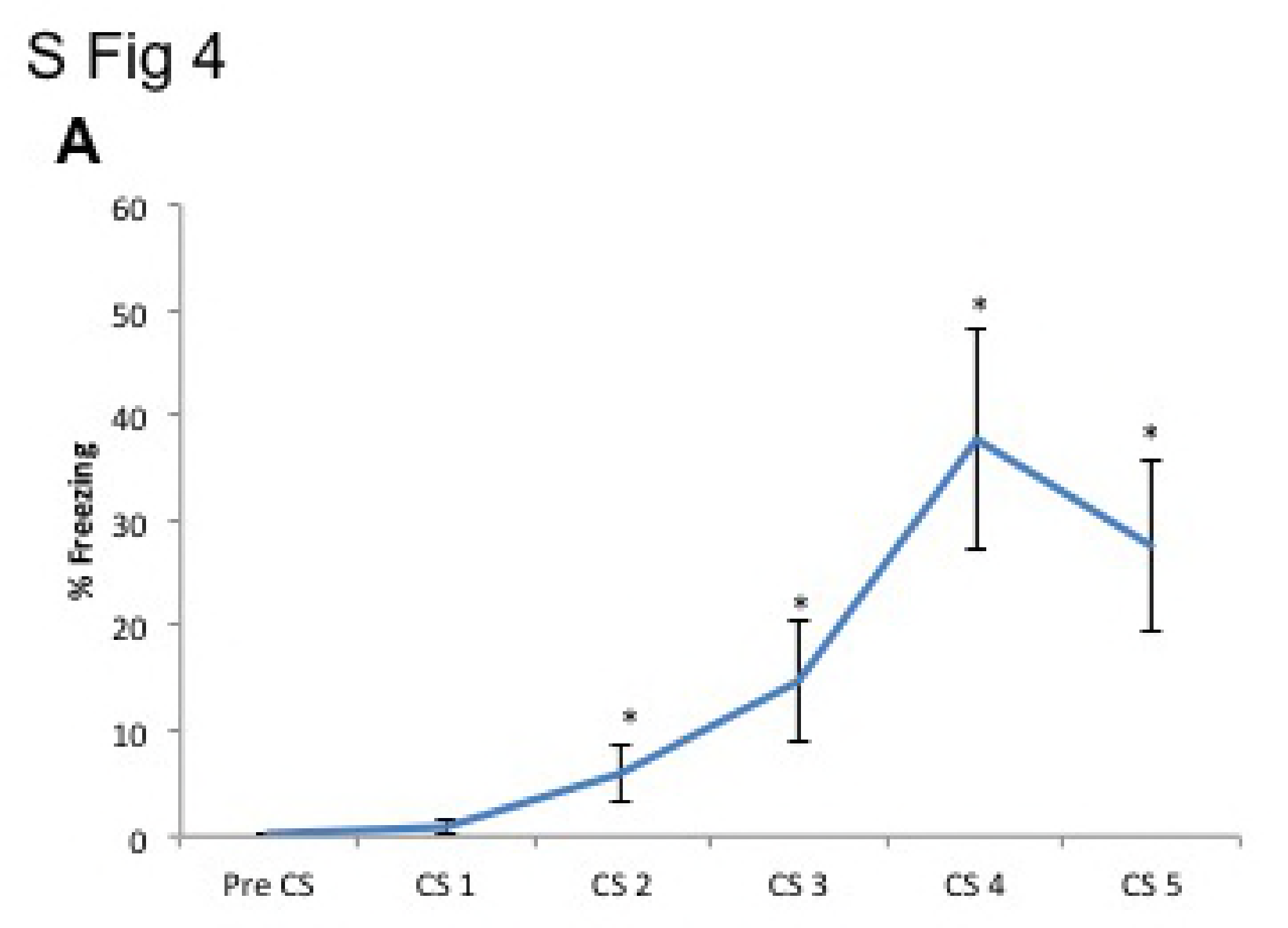

S fig 5

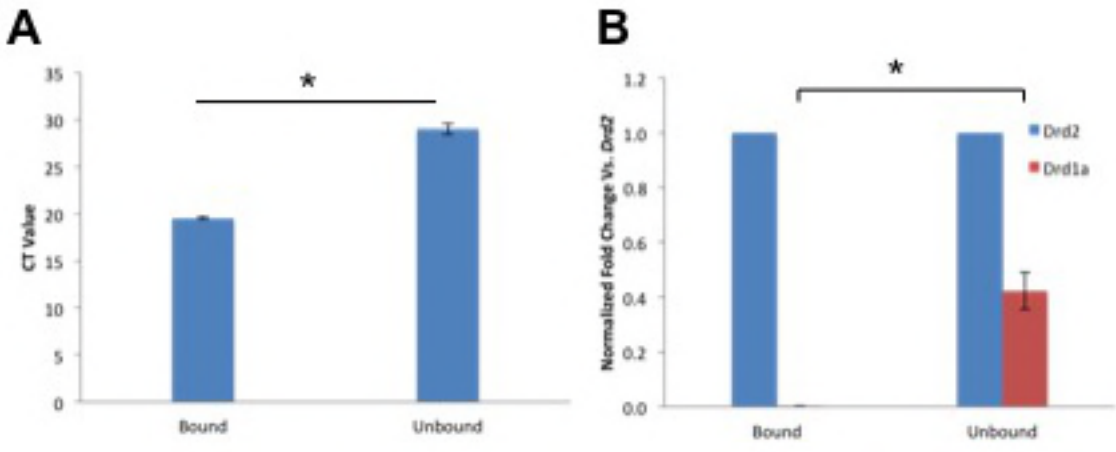
A
35
30
25
20
15
10
5
0
CT Value
*
Bound
Unbound
B
1.2
1.0
0.8
0.6
0.4
0.2
0.0
Normalized Fold Change Vs. Drd2
*
Drd2
Drd1a
Bound
Unbound

S Figure 6

A

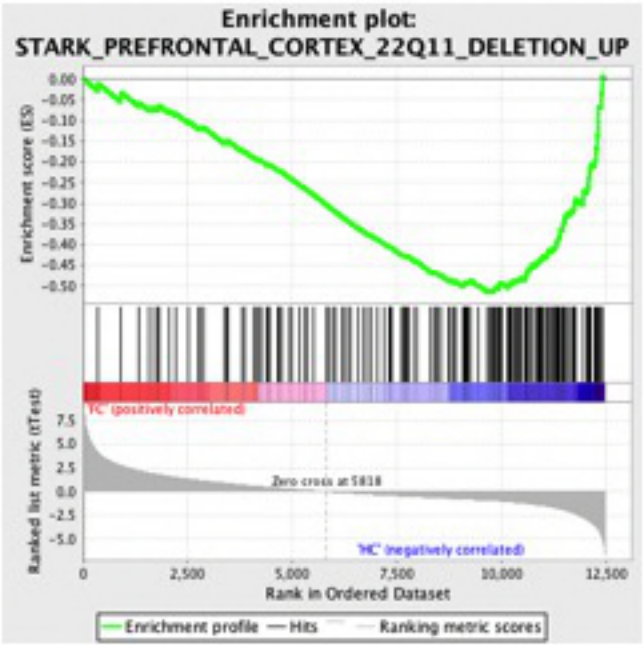
Enrichment plot:
STARK_PREFRONTAL_CORTEX_22Q11_DELETION_UP
Enrichment score (ES)
0.00
-0.05
-0.10
-0.15
-0.20
-0.25
-0.30
-0.35
-0.40
-0.45
-0.50
'TC' (positively correlated)
Ranked list metric (tTest)
7.5
5.0
2.5
0.0
-2.5
-5.0
Zero cross at 5818
'HC' (negatively correlated)
0
2,500
5,000
7,500
10,000
12,500
Rank in Ordered Dataset
Enrichment profile
Hits
Ranking metric scores

B

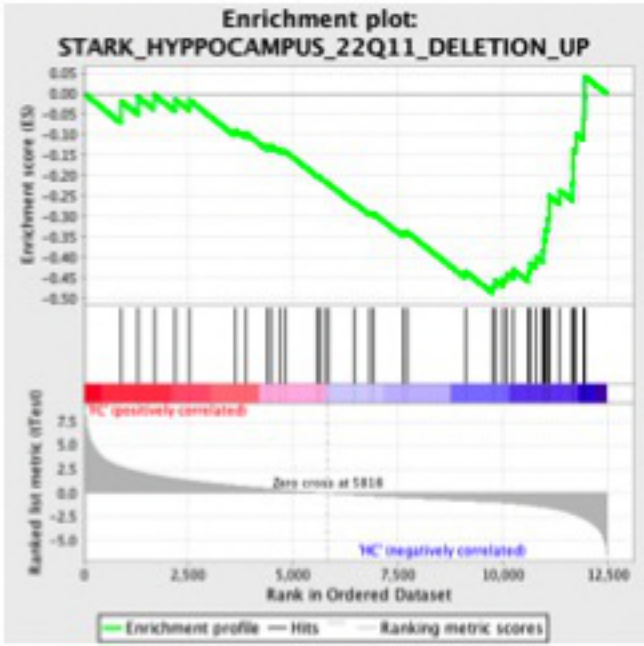
Enrichment plot:
STARK_HYPPOCAMPUS_22Q11_DELETION_UP
Enrichment score (ES)
0.05
0.00
-0.05
-0.10
-0.15
-0.20
-0.25
-0.30
-0.35
-0.40
-0.45
-0.50
'TC' (positively correlated)
Ranked list metric (tTest)
7.5
5.0
2.5
0.0
-2.5
-5.0
Zero cross at 5816
'HC' (negatively correlated)
0
2,500
5,000
7,500
10,000
12,500
Rank in Ordered Dataset
Enrichment profile
Hits
Ranking metric scores

S Fig 7

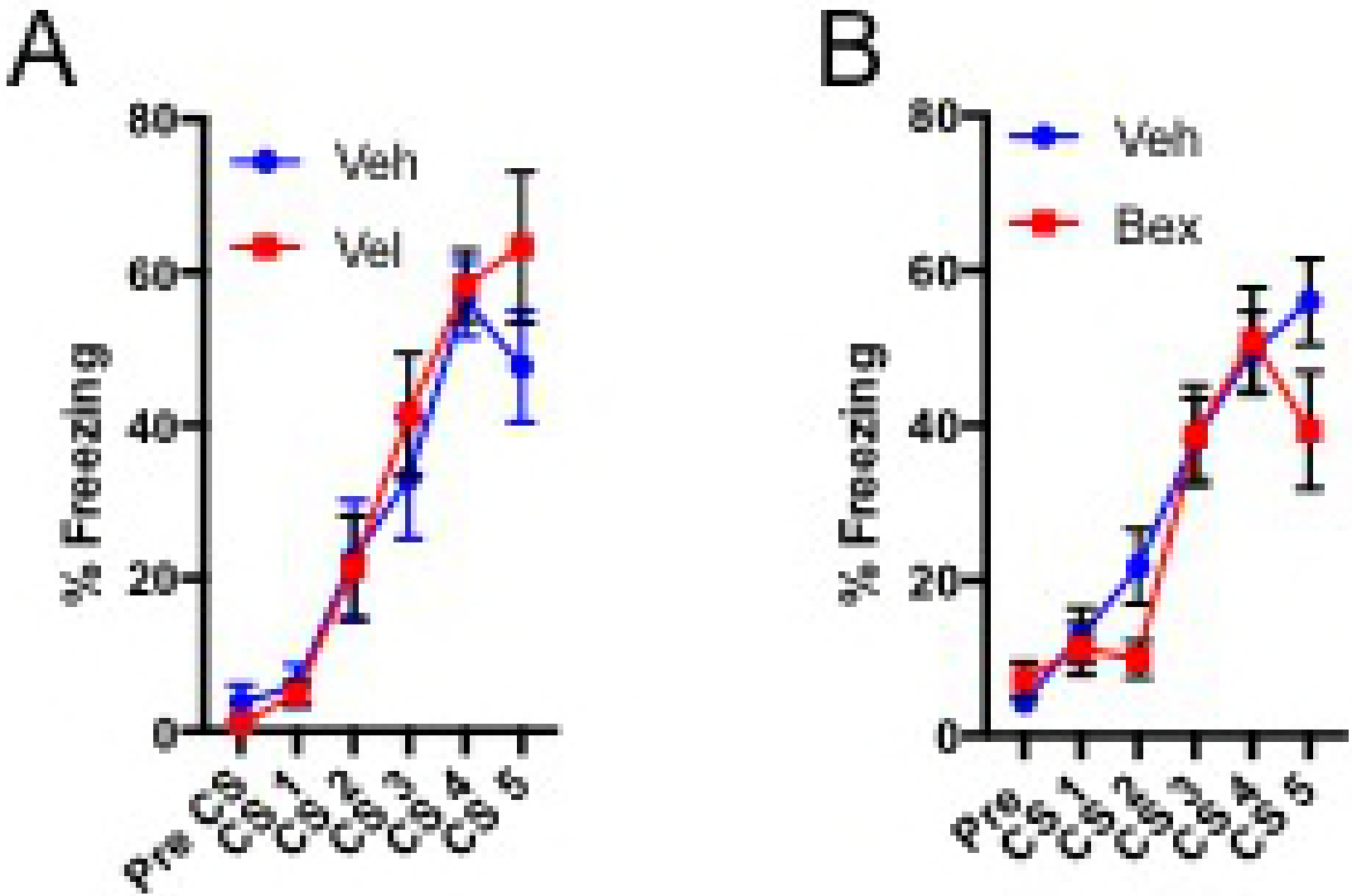

S Fig 8

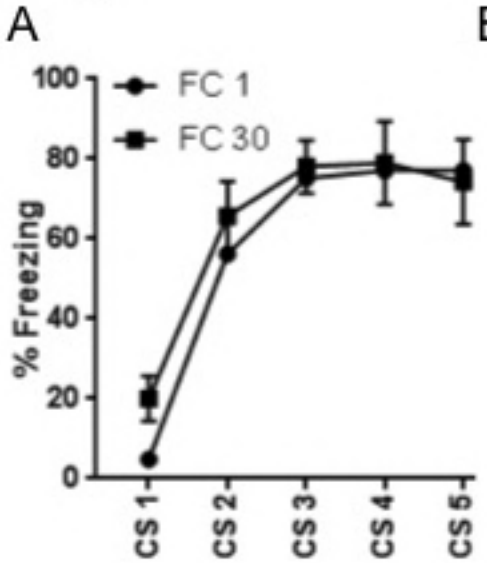
A
FC 1
FC 30
% Freezing
100
80
60
40
20
0
CS 1
CS 2
CS 3
CS 4
CS 5

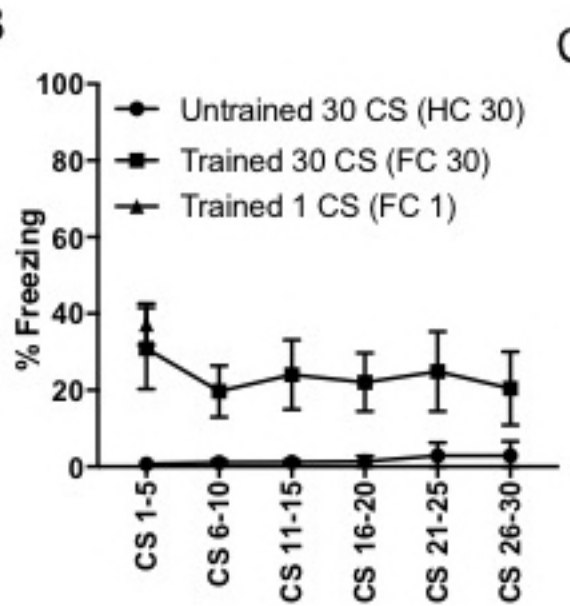
B
Untrained 30 CS (HC 30)
Trained 30 CS (FC 30)
Trained 1 CS (FC 1)
% Freezing
100
80
60
40
20
0
CS 1-5
CS 6-10
CS 11-15
CS 16-20
CS 21-25
CS 26-30

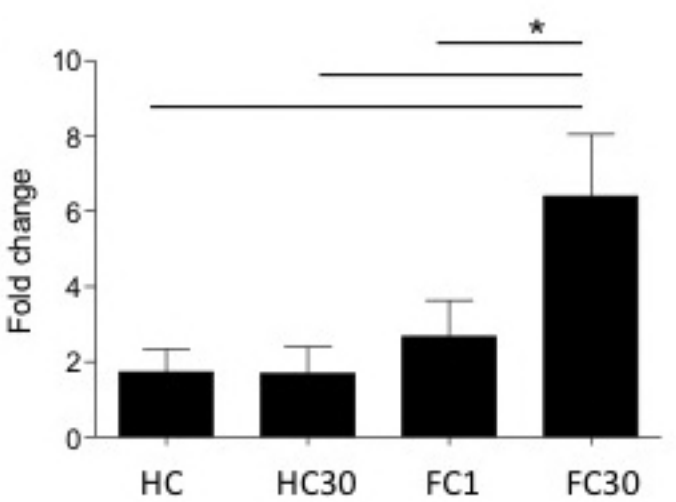
C
Fold change
10
8
6
4
2
0
*
HC
HC30
FC1
FC30

A

Name	logFC	FDR	Name	logFC	FDR	Name	logFC	FDR
Enpp2	-3.84201	5.78E-14	Mon1b	10.09996	0.035	Sstr5	9.99542	0.035
Xist	-9.00065	2.07E-10	Ralgapa1	-1.52731	0.035	[illegible]	9.93866	0.035
Fam70a	-2.54132	0.0002	Syt6	1.871516	0.023	Gpr6	1.488349	0.035
Ttr	-7.18719	0.0002	Tmem198	1.850237	0.023	B3galt5	4.806283	0.035
Gprin3	11.75968	0.0004	Impa2	8.545136	0.025	Plp1	-1.73191	0.036
Tspan2	-2.09415	0.0004	Ppp1cc	1.821304	0.025	Slc9a2	9.93478	0.036
Chl1	-2.17683	0.0005	Ddit4l	4.142671	0.026	Atp1b2	-1.42967	0.036
Nr2f2	-2.69399	0.001	C77370	-2.3852	0.026	Rxrg	1.520096	0.036
Slc1a2	-1.99747	0.001	Raver2	7.27838	0.026	Wrn	9.904032	0.036
Gpsm2	11.3125	0.003	Ccm2	1.509674	0.027	[illegible]	9.890589	0.037
Lrrc10b	2.271851	0.003	Ids	-1.57639	0.028	Ssh3	-8.03483	0.037
Atp2b4	-1.89621	0.003	Fkbp14	8.283429	0.029	Nwd1	-3.14705	0.038
Erbb4	-3.14629	0.003	30400D12F	-4.38589	0.029	Rassf7	9.885989	0.038
Tcf4	-1.70853	0.003	Adora2a	1.810633	0.029	Akap13	-2.85931	0.040
Spon1	-1.91223	0.003	Agpat1	1.636563	0.029	Calml4	-6.92224	0.040
Opcml	-2.12692	0.006	Arid2	-1.90658	0.029	Defb11	-9.43636	0.040
Vsnl1	-2.28058	0.006	Art3	10.20486	0.029	Dnalc1	-1.75625	0.040
Hpca	1.635464	0.007	Clec12a	10.11385	0.029	Etl4	-1.95632	0.040
Usp34	-2.19602	0.011	Dlgap1	-1.49759	0.029	NpySr	8.164163	0.040
Fbxo32	10.9257	0.011	Dlk1	-3.49069	0.029	Meg3	-1.4661	0.041
Kcnj13	-7.88324	0.014	Dnajc6	-1.66836	0.029	Slc44a2	-2.18456	0.041
Gm11614	-7.86926	0.016	Fbxw4	8.352591	0.029	Gpr34	9.844729	0.041
[illegible]	-1.63115	0.016	Kif1b	-1.41393	0.029	Pcdhb19	9.776541	0.041
Ednrb	-2.3345	0.016	Uhfpl5	10.20412	0.029	Carf	9.831527	0.042
Magel2	-3.99208	0.016	Mcf2l	-1.60925	0.029	Postn	9.77011	0.042
Nfia	-2.32267	0.016	Nudt18	1.552134	0.029	Tmem90a	1.583678	0.042
Plxna2	-1.75012	0.016	Pcdh8	-2.11819	0.029	Harbi1	5.964751	0.043
Smg1	-2.28151	0.018	Pnck	-1.44148	0.029	Ncapg	-8.18609	0.043
Marcksl1	-2.21668	0.018	Rictor	-2.34029	0.029	[illegible]	-1.56944	0.043
Sphkap	-1.8414	0.018	Rnf152	-4.22453	0.029	Ptprs	-1.24882	0.043
Megf9	-2.07003	0.018	Stmn4	1.423778	0.029	Slc16a2	-2.05637	0.044
Snhg11	-1.6854	0.020	Tiam2	1.552817	0.029	Grn	-1.77487	0.045
Adcy1	-1.51588	0.020	Zfp882	10.14049	0.029	Slc17a8	9.972383	0.045
C1s	-8.2976	0.020	Zscan12	6.829434	0.029	Celsr2	-1.62259	0.045
Cldn11	-3.32185	0.020	Pgm2l1	-1.3644	0.030	Gm11737	-10.7914	0.045
Epas1	-2.37535	0.020	Serinc5	-2.06885	0.030	Dll1	9.681731	0.046
Fblim1	8.489157	0.020	Apc	-1.47429	0.030	Spata2l	1.518344	0.046
Gdpd5	3.16558	0.020	Ppp1ca	1.502453	0.030	Nfib	-1.89733	0.046
Gng2	-1.6153	0.020	Zfp870	10.08861	0.030	Bcan	-1.39902	0.047
Mir5102	3.159118	0.020	Tnfsf10	-5.88709	0.031	Cyp2c44	9.653368	0.047
Tonsl	-4.36104	0.020	Fam107a	-1.54503	0.031	Leng8	-1.65006	0.047
Me1	-2.29058	0.021	Gda	-1.50518	0.031	Olp5	9.699668	0.047
Tanc2	-1.69632	0.021	Sostdc1	-4.9921	0.031	Prpf31	1.836893	0.047
Ptprt	-2.25326	0.022	Uty	8.23082	0.031	Tubb2a	-1.2474	0.047
Ly6c1	-3.6884	0.023	[illegible]	10.02666	0.032	Zfp174	9.619401	0.049
Csmd3	-2.19359	0.023	Zfp786	9.983813	0.034	Pter	-2.13507	0.049
Fgf3	3.802874	0.023	Epha5	-1.50219	0.035	Sez6l	-1.76403	0.050
Parva	-2.20091	0.023	Mblac2	-1.89384	0.035			

S Table 2

Term	Overlap	P-value	Adjusted P-value	Old P-value	Old Adjusted P-value	Z-score	Combined Score
Amygdala	14/308	7.61947E-05	0.005943189	3.56665E-05	0.002781986	-1.803188608	17.09822794
Hypothalamus	13/296	0.000284941	0.011112699	0.000143621	0.005601214	-1.57831629	12.88415638
Cerebral Cortex	12/349	0.003674422	0.095534985	0.002004113	0.052106935	-1.724255463	9.666795659

S Table 3

Term	Overlap	P-value	Adjusted P-value	Old P-value	Old Adjusted P-value	Z-score	Combined Score	Genes
Neuron_part	23/1287	0.0001	0.046	1.94E-05	9.98E-03	-7.14	64.45	EPHA5;NPY5
Neuron_projection	18/936	0.0001	0.046	2.77E-05	9.98E-03	-5.79	51.98	EPHA5;NPY5
MLL5-L_complex	2/7	0.0010	0.250	1.37E-03	1.98E-01	-1.29	8.83	PPP1CC;PPP1

Suplemental Table 4

Therapeutic Drug-target Interactions

#	Gene Symb	#	Drug	Effect	Pubmed
1	Rxrg		Alitretinoin intracellular	Activation	12482435...
2	Erbb4	2. 1.	Dacomitinib extracellular region	Inhibition	18089823
		2. 2.	BMS690514 extracellular region	Inhibition	17616683
		2. 3.	Canertinib extracellular region	Inhibition	9751783...
3	Sstr5		Octreotide extracellular region	Activation	
4	Tubb2a		Batabulin intracellular	Inhibition	10318945
5	Adora2a	5. 1.	Adenosine extracellular region	Activation	12570761 ...
		5. 2.	Propentofylline extracellular regi	Activation	10326835
		5. 3.	Caffeine extracellular region	Inhibition	1501234 ...
		5. 4.	Istradefylline extracellular region	Inhibition	11347973...
		5. 5.	Binodenoson extracellular region	Activation	11408544...
6	Ednrb	6. 1.	Tezosentan extracellular region	Inhibition	10411600
		6. 2.	Enrasentan extracellular region	Inhibition	8632328 ...

Secondary Drug-target Interactions

#	Gene Symb	#	Drug	Effect	Pubmed
1	Rxrg	1. 1.	Arotinoic acid extracellular regio	Unspecified	
		1. 2.	Retinoic acid intracellular	Activation	7608895...
		1. 3.	Linoleic acid intracellular	Activation	14622989...
		1. 4.	IRX4204 intracellular	Activation	11428923
		1. 5.	Docosahexaenoic acid intracellul	Activation	14622989...
		1. 6.	Bexarotene intracellular	Activation	8071941...
		1. 7.	ALRT1550 intracellular	Unspecified	
		1. 8.	Oleic acid intracellular	Activation	14622989
		1. 9.	Linolenic acid intracellular	Activation	14622989...
2	Fgf3		Heparin extracellular region	Activation	7592624...
3	Enpp2		Androstanolone extracellular reg	Activation	15525599
4	Bcan		Hyaluronic acid extracellular regi	Unspecified	12478611...
5	Grn		Heparin extracellular region	Unspecified	19755719
6	Tnfsf10	6. 1.	TIC10 intracellular	Activation	
		6. 2.	Mercaptopurine extracellular reg	Inhibition	15388785
7	Slc1a2	7. 1.	Estradiol extracellular region	Activation	15896872
		7. 2.	Glyoxal intracellular	Inhibition	15822816
		7. 3.	Docosahexaenoic acid extracellul	Activation	15777760
8	Epha5	8. 1.	Vandetanib extracellular region	Inhibition	15711537...
		8. 2.	Dabrafenib intracellular	Inhibition	
		8. 3.	Vemurafenib extracellular region	Inhibition	
		8. 4.	Ponatinib extracellular region	Inhibition	
		8. 5.	Alvocidib extracellular region	Inhibition	15711537
		8. 6.	Sapanisertib intracellular	Inhibition	
		8. 7.	Nilotinib extracellular region	Inhibition	22037378
		8. 8.	Bafetinib intracellular	Inhibition	
		8. 9.	Tivozanib extracellular region	Inhibition	
		8. 10.	Neflamapimod intracellular	Unspecified	15711537
		8. 11.	Alpelisib extracellular region	Unspecified	
		8. 12.	MLN8054 intracellular	Unspecified	22037378
9	Plp1		Retinoic acid extracellular region	Activation	14743441
10	Zfp983		Zn('2+) nucleus	Unspecified	9630514
11	Slc9a2	11. 1.	Phorbol 12-myristate 13-acetate	Activation	15976391

		11. 2.	Clonidine extracellular region	Inhibition	8244989
		11. 3.	Eniporide extracellular region	Inhibition	11277524...
		11. 4.	Cimetidine extracellular region	Inhibition	8244989...
		11. 5.	Zoniporide extracellular region	Inhibition	11277524...
		11. 6.	Cariporide intracellular	Inhibition	11277524...
12	C1s1		Nafamostat extracellular region	Inhibition	
13	Me1	13. 1.	L-Triiodothyronine extracellular r	Activation	9174159
		13. 2.	Androstanolone extracellular reg	Activation	15525599
14	Erbb4	14. 1.	Vandetanib extracellular region	Inhibition	22037377...
		14. 2.	Neratinib extracellular region	Unspecified	
		14. 3.	Nilotinib extracellular region	Inhibition	
		14. 4.	Ponatinib extracellular region	Inhibition	
		14. 5.	Icotinib extracellular region	Inhibition	
		14. 6.	Lapatinib intracellular	Inhibition	12467226...
		14. 7.	AEE788 intracellular	Inhibition	15256466
		14. 8.	Spebrutinib extracellular region	Inhibition	
		14. 9.	Acalabrutinib extracellular regior	Inhibition	
		14. 10.	Erlotinib extracellular region	Inhibition	
		14. 11.	Midostaurin extracellular region	Unspecified	19654408
		14. 12.	Afatinib extracellular region	Inhibition	22888144
		14. 13.	Osimertinib extracellular region	Inhibition	
		14. 14.	Vemurafenib extracellular region	Inhibition	
		14. 15.	GTS-21 extracellular region	Activation	10366678
		14. 16.	Poziotinib extracellular region	Inhibition	
		14. 17.	Lestaurtinib extracellular region	Inhibition	
		14. 18.	BI-2536 intracellular	Inhibition	
		14. 19.	Gefitinib extracellular region	Inhibition	
		14. 20.	CP724714 extracellular region	Unspecified	
		14. 21.	Brigatinib extracellular region	Inhibition	
		14. 22.	TG100115 intracellular	Inhibition	
		14. 23.	TAK-285 extracellular region	Inhibition	
		14. 24.	E7090 extracellular region	Inhibition	
15	Zscan12		Zn('2+) nucleus	Unspecified	12860387
16	Cyp2c44		alpha-Tocopherol intracellular	Activation	
17	Ppp1ca		Cantharidin intracellular	Inhibition	
18	Vsnl1	18. 1.	Mg('2+) cytoplasm	Unspecified	7806504
		18. 2.	Ca('2+) cytosol	Activation	12202488
19	Ttr	19. 1.	Furosemide extracellular region	Inhibition	9784876
		19. 2.	Flufenamic acid extracellular regi	Unspecified	9784876...
		19. 3.	Salsalate extracellular region	Inhibition	10319941
		19. 4.	Curcumin intracellular	Unspecified	19268650
		19. 5.	Trifluoperazine extracellular regi	Inhibition	9784876
		19. 6.	Diclofenac extracellular region	Inhibition	14968122...
		19. 7.	Trimethoprim extracellular regio	Inhibition	9784876
		19. 8.	Nitrendipine extracellular region	Inhibition	9784876
		19. 9.	Sobetirome intracellular	Unspecified	20937391
		19. 10.	Milrinone intracellular	Unspecified	
		19. 11.	Flurbiprofen extracellular region	Unspecified	
		19. 12.	Fluoxetine extracellular region	Inhibition	9784876
		19. 13.	Dimethyl sulfoxide intracellular	Unspecified	
		19. 14.	Tafamidis extracellular region	Unspecified	
		19. 15.	Diflunisal extracellular region	Inhibition	15080795
		19. 16.	Felbinac intracellular	Inhibition	9784876

		19. 17.	Iododoxorubicin intracellular	Inhibition	
		19. 18.	cinchophen extracellular region	Inhibition	9784876
20	Sstr5		Astemizole extracellular region	Unspecified	
21	Zfp174		Zn('2+) nucleus	Unspecified	7673192
22	Hpca		Ca('2+) cytosol	Activation	20980592...
23	Tubb2a	23. 1.	Vincristine intracellular	Inhibition	2479219...
		23. 2.	Vinblastine intracellular	Inhibition	
		23. 3.	T607 intracellular	Inhibition	16133796
		23. 4.	Estramustine intracellular	Unspecified	9020786
24	Ptprs		Alendronic acid extracellular regi	Inhibition	
25	Adora2a	25. 1.	Genistein extracellular region	Inhibition	5850...
		25. 2.	Nifedipine extracellular region	Inhibition	8709132...
		25. 3.	Regadenoson extracellular regior	Activation	11408544...
		25. 4.	Sildenafil intracellular	Unspecified	
		25. 5.	Amiloride extracellular region	Inhibition	10927025...
		25. 6.	Nimodipine extracellular region	Unspecified	8709132
		25. 7.	Clofarabine extracellular region	Activation	
		25. 8.	Trabodenoson extracellular regio	Unspecified	
		25. 9.	Quercetin extracellular region	Inhibition	8576921...
		25. 10.	Namodenoson extracellular regic	Activation	12930138...
		25. 11.	Imiquimod extracellular region	Inhibition	16575388
		25. 12.	Preladenant extracellular region	Inhibition	17236762...
		25. 13.	CEP-11981 extracellular region	Unspecified	
		25. 14.	Theophylline intracellular	Inhibition	16789747...
		25. 15.	Rolipram intracellular	Inhibition	2374150
		25. 16.	KFM-19 extracellular region	Inhibition	1404238...
		25. 17.	Isobutylmethylxanthine intracellu	Inhibition	2213834...
		25. 18.	Cladribine extracellular region	Activation	7707320
		25. 19.	Piclidenoson extracellular region	Activation	9258366...
		25. 20.	Apaxifylline extracellular region	Inhibition	11515591
		25. 21.	(RS)-Niguldipine extracellular reg	Inhibition	8709132
		25. 22.	Vidarabine extracellular region	Activation	12570759...
		25. 23.	Sonedenoson extracellular regior	Activation	11170643
		25. 24.	Fludarabine extracellular region	Inhibition	7707320
		25. 25.	Selodenoson extracellular region	Unspecified	
		25. 26.	PF-04447943 intracellular	Unspecified	
		25. 27.	FR166124 extracellular region	Inhibition	10450966...
		25. 28.	Papaverine intracellular	Inhibition	12369967
		25. 29.	Etazolate extracellular region	Inhibition	2829919
		25. 30.	GW328267 extracellular region	Activation	15267242
		25. 31.	Nicardipine extracellular region	Unspecified	8709132
		25. 32.	DPCPX extracellular region	Inhibition	1404238..
		25. 33.	Tonapofylline extracellular regior	Inhibition	17125264...
		25. 34.	Rolofylline extracellular region	Inhibition	1404238...
		25. 35.	ASP5854 extracellular region	Inhibition	
		25. 36.	Theobromine extracellular regior	Inhibition	2213834, 8230124
		25. 37.	CVT6883 extracellular region	Unspecified	18321039
		25. 38.	Niguldipine extracellular region	Inhibition	10447949
		25. 39.	Capadenoson extracellular regior	Activation	
		25. 40.	Enprofylline intracellular	Unspecified	10496952
		25. 41.	Tracazolate extracellular region	Inhibition	2829919
		25. 42.	Apadenoson extracellular region	Activation	11226132
		25. 43.	UK-432097 extracellular region	Activation	19501510...

		25. 44.	Nitrendipine extracellular region	Unspecified	8709132
26	Npy5r	26. 1.	Velneperit extracellular region	Inhibition	21545413
		26. 2.	MK-0557 extracellular region	Unspecified	
27	Atp2b4	27. 1.	Pimozide extracellular region	Inhibition	11440077
		27. 2.	Chlorpromazine extracellular reg	Inhibition	11440077
		27. 3.	Ritodrine extracellular region	Inhibition	9735158
28	Slc17a8	28. 1.	Bromocriptine intracellular	Inhibition	17662605
		28. 2.	L-Cysteine intracellular	Inhibition	16101493
29	Adcy1	29. 1.	Loratadine extracellular region	Activation	
		29. 2.	Li('+) extracellular region	Activation	
		29. 3.	Carbamazepine extracellular regi	Inhibition	
		29. 4.	DPCPX extracellular region	Inhibition	1548682
30	Ednrb	30. 1.	Bosentan extracellular region	Unspecified	11383615...
		30. 2.	L-746,072 extracellular region	Inhibition	12190306
		30. 3.	Atrasentan extracellular region	Inhibition	8676339...
		30. 4.	BMS-193884 extracellular region	Inhibition	10956219...
		30. 5.	Ambrisentan extracellular region	Inhibition	15139756
		30. 6.	Sitaxentan extracellular region	Inhibition	9171878...
		30. 7.	Macitentan intracellular	Inhibition	18780830...
		30. 8.	BQ123 extracellular region	Unspecified	
		30. 9.	PF-04447943 intracellular	Unspecified	
		30. 10.	Estradiol extracellular region	Inhibition	12967949
		30. 11.	Clazosentan extracellular region	Inhibition	9703472
		30. 12.	Tinoridine intracellular	Inhibition	16039654
		30. 13.	Sulfafurazole extracellular region	Inhibition	
		30. 14.	Darusentan extracellular region	Inhibition	11755336...
		30. 15.	Nebentan extracellular region	Unspecified	11597477...
		30. 16.	SB209670 extracellular region	Inhibition	11139453
31	Epas1	31. 1.	Co('2+) nucleus	Activation	11688986...
		31. 2.	Firtecan pegol intracellular	Inhibition	
		31. 3.	PT2385 intracellular	Inhibition	
32	Nfia		Androstanolone extracellular reg	Inhibition	15525599
33	Kcnj13	33. 1.	Terikalant intracellular	Inhibition	9763763...
		33. 2.	Pimozide extracellular region	Inhibition	
		33. 3.	Ketoconazole extracellular regior	Inhibition	
		33. 4.	Prazepine extracellular region	Inhibition	
		33. 5.	Dofetilide extracellular region	Inhibition	593709...
		33. 6.	Haloperidol extracellular region	Inhibition	
		33. 7.	Cisapride extracellular region	Inhibition	
		33. 8.	Sertindole extracellular region	Inhibition	
		33. 9.	Ambasilide intracellular	Inhibition	10226864